SCOUR AROUND PIERS AND ABUTMENTS: PREDICTION OF GRIP LENGTH

by

AJAY KUMAR SINGH

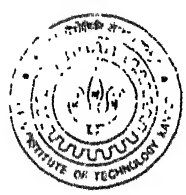

DEPARTMENT OF CIVIL ENGINEERING

INDIAN INSTITUTE OF TECHNOLOGY, KANPUR

July, 2002

SCOUR AROUND PIERS AND ABUTMENTS: PREDICTION OF GRIP LENGTH

A Thesis submitted

In Partial Fulfillment of the Requirements

For the Degree of

MASTER OF TECHNOLOGY

by

AJAY KUMAR SINGH

to the

DEPARTMENT OF CIVIL ENGINEERING

INDIAN INSTITUTE OF TECHNOLOGY, KANPUR

July, 2002

CERTIFICATE

It is certified that the work presented in this thesis entitled **"Scour around piers and abutments: Prediction of grip length"** by **Ajay Kumar Singh,** has been carried out under our supervision in partial fullment of the requirement for the award of M.Tech. Degree in Civil Engineering. This thesis is a record of bonafide work carried out in the Department of Civil Engineering, I.I.T. Kanpur during the year 2001-2002 and this work has not submitted elsewhere for a degree.

Dr. T. Gangadharaiah
Professor
Department of Civil Engineering
Indian Institute of Technology,
Kanpur.

Dr. P.K. Basudhar
Professor
Department of Civil Engineering
Indian Institute of Technology,
Kanpur.

July, 2002

Dedicated

to

my elder brother

ABSTRACT

The thesis pertains to the experimental studies of the effect of the scouring of river beds on the stability of piers and abutments. Two types of river sand (Yamuna and Ganga) were used in the experiments to study the effect of average particle size diameter (d_{50}). Scouring pattern was observed around the above type of foundation under varying embedment depth, flow depth and Froude number. Linear and non-linear regression analysis of the data thus generated have been carried out using STATISTICA package. The obtained relations show the good to excellent correlations.

Theoretical model to predict the grip length at the limiting equilibrium state has been developed. The predictions regarding the scour depth needed in the above equations were made using the relation obtained from the regression analysis as mentioned above. Thus the method of prediction is the semi empirical one. The predictions made regarding the grip length uses the above theory were compared with experimental values. The comparison had shown good to excellent agreement when the embedment depth ratio (H_E/D) was greater than 2. The goodness ratio defined as the ratio of the theoretically predicted values of grip length ratio (G_l/h) to that obtained from the experimental observations ranges from 1.13 to 1.67 for the embedment depth ratio (H_E/D) greater than 2. However for embedment depth ratio (H_E/D) less than 2 predictions made were very poor.

Acknowledgements

I feel highly indebted to my thesis supervisors Prof. P.K.Basudhar and Prof. T. Gangadharaiah for their most efficient and invaluable guidance at every stage of my thesis work. I am enriched with the practical side as well as theoretical of the work through their scholarly guidance, constructive suggestions, critical comments and detailed instructions at every stage.

I would like to express my deep sense of gratitude to my respected Professors Dr. M.R.Madhav, Dr. N.S.V.Kameshwara Rao, Dr. P.K. Basudhar, Dr.Sarvesh Chandra and Dr. Umesh Dayal for giving me an exposure and professional knowledge in the field of Geotechnical engineering.

The help rendered by Mr. P.Jagannathan, Mr. Manoj Kumar, Mr.J.P.Pandey, Mr. Sitaram, the members of hydraulics lab and Mr. R.P.Trivedi, Mr. A .K. Srivastava, Mr. Gulabchand, the members of Geotechnical engineering laboratory were deeply acknowledged.

Special thanks to my senior Prashant Mamgain and my classmates Imran, Avinash, Habibul Rahman, Keshav, Uma, Gupta, Neha, Dhanunjay, Shekhar, Venkat Rao and Nageshwar Rao who made my stay at IIT Kanpur a pleasant one.

I am thankful to my friends Pankaj, Kishore, Prabhakar, Dharmesh, Manoj, Preeti Maheshwari, Meenu Kapil, Ajeet, Santosh, Anirudh, Rajinikant, Amit, Kanchan Kumar, Wasif, Rawat and Shahab for their valuable suggestions and help during my thesis.

I am thankful to my friends Aditya, Ajay, Pushpendra, Kuldeep, Mahipal, Dinesh, Ashok, Kamlesh, Amit, Kundan, Ashish and Vikas for their constant encouragement during my Bachelor and Master's degree programme.

Finally I would like to express my gratitude to my parents and family members for their encouragement to do postgraduate studies and their support at all the times.

Ajay Kumar Singh

CONTENTS

List of Figures

List of Tables

List of Notations

β	Exponent of D for peir size effect
ρ	Unit weight of water
σ_g	Geometric standard deviation
ρ_s	Unit weight of soil
γ_s'	Submerged density of soil
B	Width of channel
C_D	Drag coefficient
D	Diameter of circular peir, width of oblong peir, sides of square abutment
d_{50}	Size for which 50% of sediment by weight is finer
d_m	Mean size of the sediment in mm
D_{se}	Scour depth measured below the water surface
f	Lacey's silt factor
F_r	Froude number
F_R	Modified Froude number
F_s	Soil resisting force
F_w	Force due to water current
G_l	Grip length at the failure condition
h	Flow depth
H_E	Embedment depth of pile below the sediment bed level
H_m	Lacey's regime depth
hs	Maximum scour depth with respect to original bed level
K_d	Sediment size multiplying factor
K_p	Coefficient of passive earth pressure
Q	Design flood discharge in m^3/sec
q	Discharge intensity
U	Mean velocity of flow

W	Combined weight of superstructure and peir
w_l	Weight of the super structure
w_s	Weight of peir
y	Distance of F_w from foundation base

CHAPTER 1

INTRODUCTION

1.1 General

Rivers are natural flowing phenomenon. Bridges across rivers obstructs the flow, due to flow disturbances induced by the bridge piers, abutments causes a decrease in bed elevation adjacent to the piers or abutments. This abrupt decrease in bed elevation near a pier or abutment due to erosion of bed material by the flow is known as local scour. Cause of local scour is the formation of horseshoe vortex at the bed pier junction. Excessive scour can lead to instability and collapse of structure.

Scour around bridge foundation has been the subject of many investigators and scour problem is investigated extensively by experimental work with laboratory models by Tison(1940), Laurson and Toch (1956), Chabert and Engeldinger (1956), Larras (1965), Neill (1964), Paintal and Garde (1965), Shen and Schneider (1970), Melvill (1975), Baker (1979,80,81), Raudviki (1990), Garde and Kothyari (1995), Shepperd et. al. (1998). Their contribution is towards the prediction of scour depth under different conditions.

1.2 Thesis presentation

The thesis is being presented in five chapters:

(1) Introduction and review of literature.

(2) Experimental details.

(3) Experimental results and discussion.

(4) Theoretical prediction and comparison with experimental results.

(5) Conclusion.

1.3 Review of Literature

Brief literature are presented here:

1.3.1 Cause of scour

Scouring phenomenon is due to shear stress exerted on the bed by the flowing water that causes the motion of sediment bed. After the sediment bed attain equilibrium and the obstruction is placed, the alluvial around the obstruction changes due to shear distribution.

Down flow in front of the obstruction acts like vertical jet eroding the bed in front of the pier and turns 180^0 near the bed and the upward flow is deflected by the horseshoe vortex in the upstream direction up the slope of the scour hole.

Obstruction induces an adverse pressure gradient in the flow resulting in a3-dimensional boundary layer separation in front of the pier near bed. This causes the formation of a system of vortices, which wrap around the pier in the shape of a horseshoe in plan.

Thus scour is caused by a system of vortices in cohesionless alluvium due to a 3-dimensional boundary layer separation, and the variation of scour hole depth with time depends on size of obstruction, bed material and the hydraulic parameters.

1.3.2 Mechanism of scour

The process of scour around river structures such as bridge piers etc. involve lot of complexities of the 3-dimensional flow and sediment interaction. The scour, the flow pattern and the rate of scouring change with time and condition until steady flow condition are re-established at the equilibrium stage. Formation of local scour occurs due to adverse pressure gradient resulting in boundary layer separation of flow near the bed level at certain distance ahead of the structure. The separated flow then coil up to form the primary vortex, also designated in case of piers as scouring horseshoe vortex. Scouring occurs if the shear stress generated by the vortex is stronger than that required for the entrainment of the bed material.

The vortex together with the down-flow provides a dominating scouring mechanism.

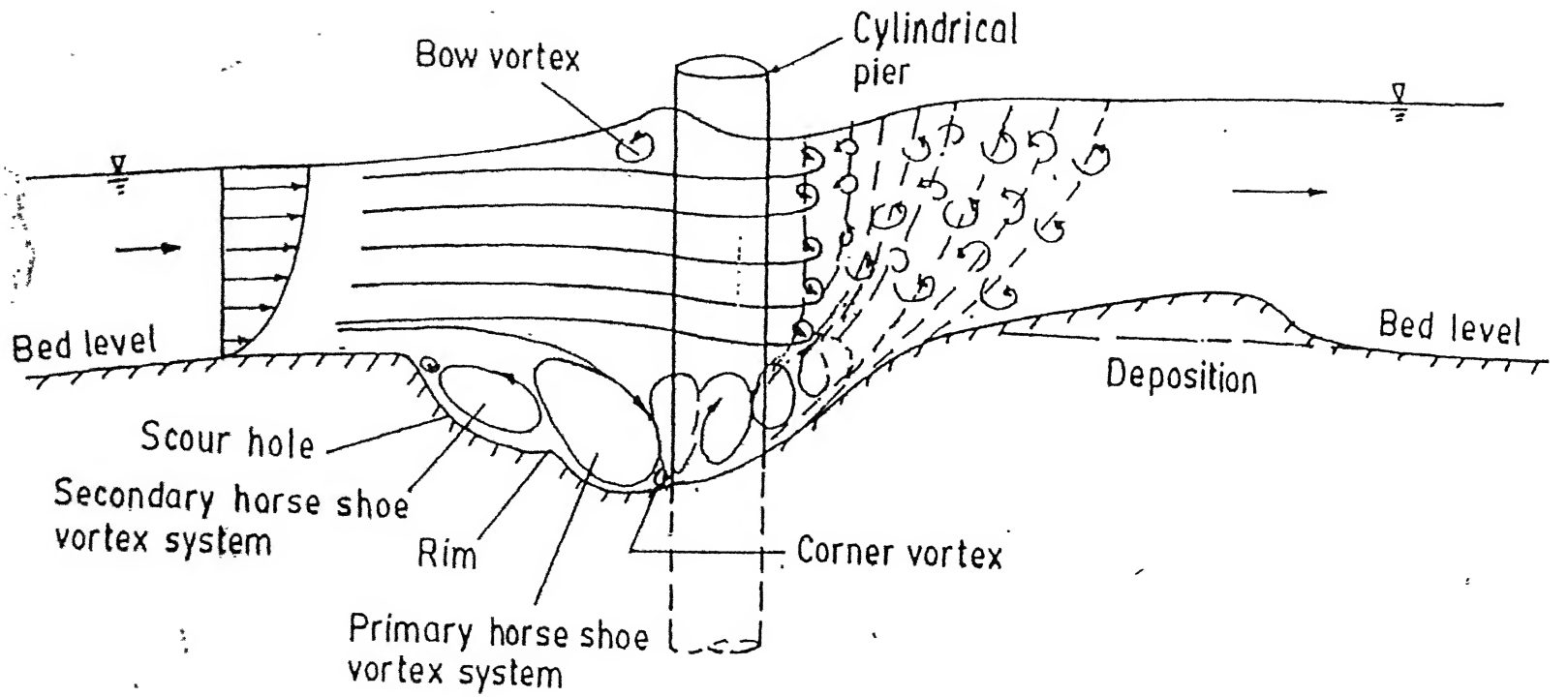

Fig. 1.1: Horseshoe Vortex on mobile bed: Longitudinal sectional sectional view

When a cylindrical pier or pile is held perpendicular to the flow, an adverse pressure gradient in the direction of the flow develops in its vicinity if the pier and this result in separation and rolling up of the approach flow. The rolled vortex is swept downstream around the pier this vortex is called 'horseshoe vortex' Melville (1975) noted that, the horseshoe vortex is initially small in cross-section and is comparatively weak. With the formation of scour hole, the vortex rapidly grows in size and strength as additional fluid attains a downward component and the strength of the down-flow increases. The down-flow acts somewhat like a vertical jet in eroding the bed. As the scour hole enlarges, the circulation associated with the horseshoe vortex increase being controlled by the quantity of fluid supplied to the vortex via the down-flow ahead of cylinder. This in-turn is determined by the discharge of the approach flow or for a particular flow depth and width, by the magnitude of the velocity of the approach flow. The magnitude of the down-flow near the bottom of the scour hole decreases as the depth of the hole increases. Hence the rate of erosion decreases. The armor coat, if present, helps to limit. Erosion. At a certain stage equilibrium is reached. The combination of temporal mean bed shear and the turbulent agitation near the bed becomes incapable of removing further bed material from the scour area ahead of the cylinder and in the lower portion of the scour hole. Hence equilibrium is a condition at which the depth of scour ahead of the cylinder is just sufficient so that the magnitude of the vertically downward flow ahead of the cylinder can no longer dislodge surface grains at the bed. The horseshoe vortex and scouring phenomenon around cylindrical pier is shown in Fig1.1.

A number of investigators like Larsen and Toch (1956), Roper et al. (1967), Baker (1981), Kothyari(1989), Muzzamil and Gangadharaiah (1995), considered the horseshoe vortex as the basic cause of local scour.

1.3.3 Scour depth prediction

Estimation of correct depth of scour at the bridge below the ambient stream bed is very important since that determines the depth of foundation for the pier. Estimation of scour depth is very much important for the geotechnical aspect of design. For the estimation of local scour depth at bridge piers, many formulae have been proposed and these formulas is based on different approaches. Some of better-known formula is presented here.

Inglis et al. (1939) carried out model studies on piers in connection with the Hardinge Bridge works over river Ganga. They found that scour depth could be expressed as:

$$\frac{h_s}{D} = 2.32\left[\frac{q^{2/3}}{D}\right]^{0.78}$$

where

h_s = scour depth measured below the sediment bed level

D = diameter of the pier

q = discharge intensity in m^3/sec/m

A major disadvantage of this relation is the combination of undisturbed water depth and scour depth. The formula was later modified using regime depth relation by Blench (1962) and Arunachalam (1967). Inglis (1949) based on the analysis of scour data on 17 bridges in the Indo-Gangetic plains proposed a formula for the scour depth,

$$D_{se} = 2\,H_m$$

where H_m is known as Lacey's regime depth given as:

$$H_m = 0.47\left[\frac{Q}{f}\right]^{1/3}$$

where,

D_{se} = scour depth measured below the water surface = $(h+h_s)$

f = Lacey's silt factor = $1.76\sqrt{d_m}$

Q = design flood discharge in m^3/sec

h = depth of flow

h_s = scour depth measured below the ambient bed level

d_m = mean size of sediment in mm

This is popularly known as Lacey-Inglis method of estimating scour depth and is recommended for use by Indian railways and Indian road congress. This method is purely empirical in nature and gives combined scour caused due to flow modification by introduction of a pier, flow constriction due to guide bunds, and flow concentration due to non-uniform distribution of flow. It is obvious from the formula, that flow depth and pier geometry are unimportant. This approach does not reveal the internal mechanism involved in the scouring pattern.

The regime equation originally derived from straight reaches of channels in equilibrium for parallel flow conditions are not applicable to flow conditions at bends and obstructions, where the flow is mainly characterized by large scale curvature, separation, vortex formation, macro-turbulence and energy dissipation.

1.3.4 Scour around piled foundation

Scouring around piers has been thoroughly investigated than that of pile groups Useful insight to this aspect of local scour is provided by an investigation by Hannah (1978), who studied local scour at groups of cylindrical piles with steady uniform flow and clear water conditions.

For scour at piled foundations, where the pile cap is clear of the water surface, Hannah (1978) found that the maximum scour depth is closely related to the dimension of the pile group as a hole, as seen from the upstream. He recommended that a single line of piles should be used in preference to piers for angle of attack greater than 8 degrees. A series of tests was first performed on single piles with a pier (length: width = 1:6) to provide a basis against which pile group scour could be evaluated. Pile group of various spacing and with different angle of attack was then investigated for one flow conditions. The sediment used in all tests had a $d_{50} = 0.75$ mm and standard $(\sigma_g) = 1.32$ tests showed that scour depths were 80% of equilibrium scour depths after seven hours. Further, after seven hours, only minor changes occurred in sour and deposition patterns. Raudviki (1990) explained the scouring pattern for the two piles in series and in transverse direction.

When the two piles are in series and are in contact the scour depth at the front pile was same as that was single pile. But with increase separation, the front pile experiences

the reinforcing effect which reaches a maximum value at a/b = 2.5 and is evident until a/b = 11. Where a is the center to center spacing between piles and b is the common pile diameter. For larger spacing, the scour depth is the same for a single pile. With larger separation (a/b = 10) between the piles, bed level increases as some of the material from the front hole is deposited between the piles. At a spacing of a/b=10, the scouring in front of second pile is balanced by deposition from the front scour hole. For larger spacing, the reinforcing effect at the from pile is weak and disappears completely as the bed profile assumes that arising, (a/b = 2), the increased scoring results from the increase effective pile diameter At a/b > 2, separate horseshoe vortices and greater scouring potential which reduces as a/b increases. Or pile cap, the footing, capping or caissons with top below the general bed level can be effective in reducing the local scour depth by interception of the down flow. However, if the top of the wider foundation element comes to bed level, or even above, the scour depth is increased.

Melville conducted the experiments for the following four cases:

(1) Top of footing below the scour hole.

(2) Top of the footing within the scour hole below the general bed level.

(3) Top of the footing above the general bed level.

(4) Where the footing is at or above the water surface level.

He concluded that for the first case, when the footing, cap or caissons buried below the scour hole base, local scour has no effect due to footing. While in the second case, local scour is reduced due to the interception of the down-flow. For the third case scour depth increases for a pier founded on a large size caisson. But for the fourth case, the maximum local scour occurs, when the top of the caisson or pile cap is at the water surface level.

Mamgain (2001) had done the experiments to find the particular arrangement of piles, suitable position of pile cap with changed flow conditions, and to estimate the scour depth develop a general equation for Yamuna river sand

1.3.5 Effect of pier shapes and sizes

Most of the bridge piers are designed with circular shape or semicircular shape on upstream and downstream end. Circular piers are defined as standard pier shape. The

extent of maximum scour depth depends on mainly the pier shape and size foe a given flow condition. The effect of pier size on scour depth is proportional, i.e. larger the size, more is the equilibrium scour depth.

Melville (1988) suggests a shape factor to account for the effect of pier shape.The opinion presented on the relationship between pier size and equilibrium scour depth is quite diverging. A conclusion that is easy to draw is that larger the size, more is the equilibrium scour depth. For all other factor being constant the scour depth varies as $D\beta$ where D is the size or width of pier and $0.5 \leq \beta \leq 1$. Breusers (1972) proposes $\beta = 1$ for $h_s = 1.4D\beta$. Laursen and Toch (1956) design curve corresponds to $\beta = 0.7$ for the equation hs = 1.35Dβh0.3, Larras (1963) suggests $\beta = 0.75$ for $h_s = 1.05$ D 0.75, where h_s is maximum scour depth around unprocted pier.

Mostafa (1994) measured local scour depths at a variety of different uniform pier shapes all having the same projected width. Result shows that the least scour depth for the same flow condition is recorded for the circular pier. Non-uniform pier include pier with pile foundations, cessions, slab footing and tapered piles. Downward tapering piers induce deeper scour than a circular pier of the same width, and vice versa. The general conclusion is that the blunter the pier the deeper the local scour. It is because, the frontal area of the pier facing the flow increases for a blunt rather than a streamlined shape.

1.3.6 Influence of constriction ratio

The constriction ratio, defined as the ratio of the width of the flume to the size of the pier, (B/D), influences the equilibrium scour depth at the piers. Shen et al (1969) suggest that, for clear water experiments, the flume width should be at least eight times the diameter or size of the pier. The same ratio for live bed scour should be at least 10 times the pier size (Chiew 1984). A flume width smaller than this is likely to reduce the scour depth, as the bed features are likely to modified as move through the constriction.

1.3.7 Influence of sediment size

Ettema (1980) and Chiew (1984) studied the influence of sediment size on scour depth at Circular piers for uniform sediments for clear water flows and live bed scour respectively. Their data show that the equilibrium scour depth in creases with the relative

sediment size (D/d_{50}) up to $D/d_{50} = 50$. For ($D/d_{50} > 50$), which is the case of most of the practical situation; H_{sm} is independent of the sediment size. Ettema explained that the reduction in scour depth for relatively large sediments were due to large particles impending the erosion process at the base of the scour hole and dissipating some of the flow energy in the erosionzone.

For non-uniform sediments ($\sigma_g \geq 1.3$) a process known as armouring occurs in the scour hole. Where σ_g represents geometrical standard deviation obtained from the logarithmic probability distribution graph. The different mobility in a mixture of particles of different diameters is responsible for armouring or paving of the channel bed. Armour layer formation in non-uniform sediments leads to reduced scour depths (Dongal, 1994;Raudkivi et. al., 1977; Wong, 1982; see juyal, 2000). The effective size of non-uniform sediments can be defined as the size of uniform material, which gets scoured at the same rate as the non-uniform material under the given conditions.

Data by Baker (1986) for pier scour in graded sediments under live bed conditions show that sediment gradation effects are considerably reduced at higher flow intensities. Melville (1992) plotted data of Wong (1982) under clear water conditions for abutments, which showed dramatic decrease in scour depth for widely graded sediments. Melville (1997) plotted pier and abutment data in terms of the semdiment size multiplying factor, K_d, which is defined as the ratio of the scour depth for a particular D/d_{50} to that for $D/d_{50} > 50$.

1.3.8 Influence of flow depth

There are conflicting views on the effect of flow depth on the local scour depth. Observation shows that at shallow flow depths, the local scour at piers increases with flow depth but as the water depth increases, the scour depth becomes almost independent of flow depth. This trend is shown by Laursen (1963), Breusers (1977), Ettema (1980), Chiew (1982). Laursen (1963) and most researchers influenced by the regime theory state that for constant velocity, the depth of scour increases with increasing water depth. The presence of a pier causes a free surface roller around the pi9er and the horseshoe vortex roller at the base of the pier. The two rollers have

opposite direction of rotation, Melville (1988). As long as they do not interfere with each other, the local scour depth is independent of flow depth.

1.3.9 Influence of angle of attack

The depth of local scour for all shapes of pier except cylindrical, is strongly dependent on the alignment to the flow. As the angle increases, the scour depth increases because the effective frontal width of the pier is increased. Melville (1977) observed that at a zero angle of attack the scour depth can be minimized by streamlining the pier, but this advantage disappears for angles of attack greater than 10^0.

1.3.10 Methods of reducing local scour

Scour protection devices have been classified in to following categories (Setia, 1997):

1. Weakening of the horseshoe vortex by providing piles upstream of piers or slot in the pier.
2. Arresting the sinking of horseshoe vortex by providing riprap material or collar plates type of devices.
3. Modifying the horseshoe vortex by providing delta-wing like passive device.

Setia's(1997) experiments reveal that each type of protection good for particular flow conditions. Combination of them is found to act as better scour protection aids.

1.3.11 Pile group effect on scour depth

Hannah (1978) (see Raudkivi, 1990) studied the local scour at group of cylindrical piles with steady uniform flow and clear-water conditions. Four types of mechanisms that occurs during scouring process when piles are arranged in a row, are described as follows:

1. Reinforcing: It causes increased scour depths at the front pile. If the downstream pile is so placed that the scour hole overlaps, then the bed level is lowered at the rear of the upstream scour hole. It is thus easier for the flow to remove material from this hole and it

deepens. As pile separation increases, the reinforcing effect reduces and disappears when the maximum bed level between the piles returns to the undisturbed bed level.

2. Sheltering: the presence of an upstream pile can cause a reduction in the effective Approach velocity for downstream piles. The reduction decreases the effect of the 'horseshoe vortex' and thereby reduces scour at downstream piles. A second form of sheltering occurs if material scoured from the upstream pile is deposited on the bed in front of the downstream pile. The strength and thus the effectiveness of the horseshoe vortex at this pile is reduced. As pile separation increases, the sheltering effect decreases.

3.Vortex shedding: Vortices shed from an upstream pile are convected downstream. When a second pile is so placed close to one of the vortex shedding paths, the vortices assists in lifting the material from the scour hole. The scoring potential of the she vortex is a function if its convection speed and of the distance between the path and the affected pile. This effect will therefore, reduce more rapidly for piles in line and for those downstream piles placed on the paths traced by vortices shed by upstream piles.

4. Horseshoe vortex compression: when piles are placed transverse to the flow, each pile will have, expect at very close spacing, its own horseshoe vortex. As pile spacing is decreased, the inner arms of the horseshoe vortices will be compressed. This causes velocities with in the arms to increases with a consequent increase in scour depths. This compression also exists for piles in staggered arrangement. Experiments were conducted by Jones (1993) to determine guidelines for specifying the characteristic width of a pile group that is or may be exposed to the flow. He concluded that, when pile groups project a above the streambed, they can be analyzed conservatively by representing them as a single width equal to the projected area of the piles ignoring the clear space between piles. Good judgment needs to be used in accounting for debris because pile groups tend to collect debris that could effectively clog the clear spaces between piles and cause the pile group to act as a much larger mass.

1.4 Objective of the present study

The embedment depth is an important factor for the safety of piers against overturning or failure caused by scouring of river bed due to increased flow in the rivers. The present study focused mainly to find the adequate embedment depth of piers and abutments with changed flow conditions, so that the safety of river crossing structures can be ensured. For this, it is necessary to estimate the scour around these structures under varying flow conditions for soils that are generally found in the river beds of the region. In this study, experiments have been conducted with Yamuna and Ganga river sand with the purpose of developing a general predictive theoretical model to estimate the scour depth. Knowing the depth of scour, it is possible to predict the necessary grip length for adequate safety and stability of such foundations. Till now no information's available in literature to estimate directly the grip length as a function of scour depth, flow depth, Froude number and d_{50}. Thus, there is a need to develop such an expression. So, in this thesis an effort has also been made to find a rational expression based on theoretical approach and experimental observations.

CHAPTER 2

EXPERIMENTAL DETAILS

Experiments were carried out in a hydraulic flume located in the Hydraulics and Water Resource Laboratory, of the Civil Engineering Department at Indian Institute of Technology, Kanpur.

Experiments were planned and designed to represent different condition that may be encountered in the field.

2.1 Experimental channel

Experiments were conducted in two glass walled channel. First glass walled channel is 8.0 meter in length, 0.40 meter in width and 0.60, meter deep. The channel was filled with Yamuna sand (d_{50} = 0.32 mm), sand bed was 0.20 meter deep and was packed with gravel curtain on up upstream and downstream ends to prevent erosion of sand at the inlet and outlet during the flow of water. A sediment trap was also provided at the end of downstream gate. Depth of flow in the flume was controlled by two gates, one at the upstream and the other at the downstream of the model. The water flow was received from an overhead tank and the discharge was measured with the help of a triangular notch provided at the end of the sediment trap. The outflow was recirculated with the help of water pumps.

Second glass walled channel is similar to first glass walled channel in shape. The size of this channel is 5 meter in length, 0.45 meter in width and 0.90 meter in depth. This channel is filled with the fine sand (Ganga river sand, d_{50} = 0.15 mm). Fine sand bed was 0.25 meter deep. This fine sand bed is packed with gravel curtain on upstream and downstream to prevent the sand getting eroded at the inlet and outlet. A sediment trap was also provided at the end of downstream. In order to maintain uniform flow depth and discharge upstream and downstream gates operated suitably. Discharge was measured with the help of a rectangular weir. An open well located 0.50 meter upstream of the weir

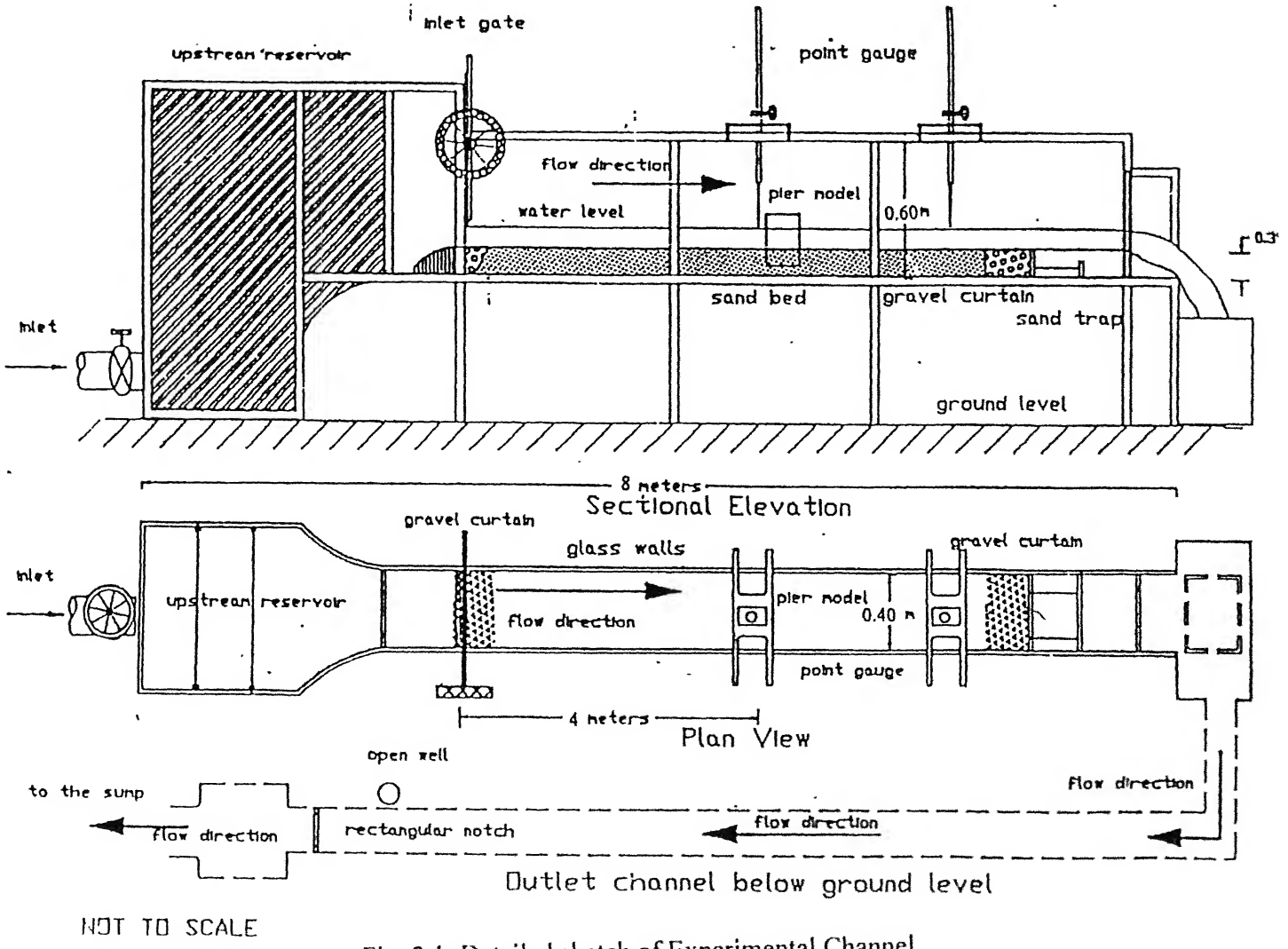

Fig. 2.1: Detailed sketch of Experimental Channel

was made use of for taking the head acting over the weir. The outflow was recirculated with the help of water pumps. The arrangement is shown in fig. 2.1.

2.2 Characteristics of sand

Yamuna river sand and Ganga river sand passing through 2 mm IS sieve has been used in conducting all the experiments. The particle size distribution curve for Yamuna river sand and Ganga river sand are shown in Fig.2.2. and Fig.2.3. resprctively.

Yamuna river sand used for experiments has the following properties:

d_{50} = 0.32 mm

Specific Gravity (G_S) = 2.66

Uniformity coefficient (C_U) = 1.76

Coefficient of curvature (C_C) = 1.01

The chosen Yamuna sand is categorized as poorly graded sand as per IS code.

Ganga river sand used for experiments has the following properties:

d_{50} = 0.15 mm

Specific Gravity (G_S) = 2.67

Uniformity coefficient (C_U) = 2.13

Coefficient of curvature (C_C) = 0.89

The chosen Ganga river sand is categorized as poorly graded sand as per IS code.

Shear strength parameters of sand (Direct shear test)

For Yamuna sand:

Placement density = 15.43 kN/m^3

Angle of internal friction for dry condition $\phi = 32.34^0$

Angle of internal friction in submerged condition $\phi' = 32^0$

Cohesion (C) =0.0

For Ganga sand:

Placement density = 15.86 kN/m^3

Angle of internal friction for dry condition $\phi = 34.01^0$

Angle of internal friction in submerged condition $\phi' = 33.68^0$

Cohesion (C) = 0.0

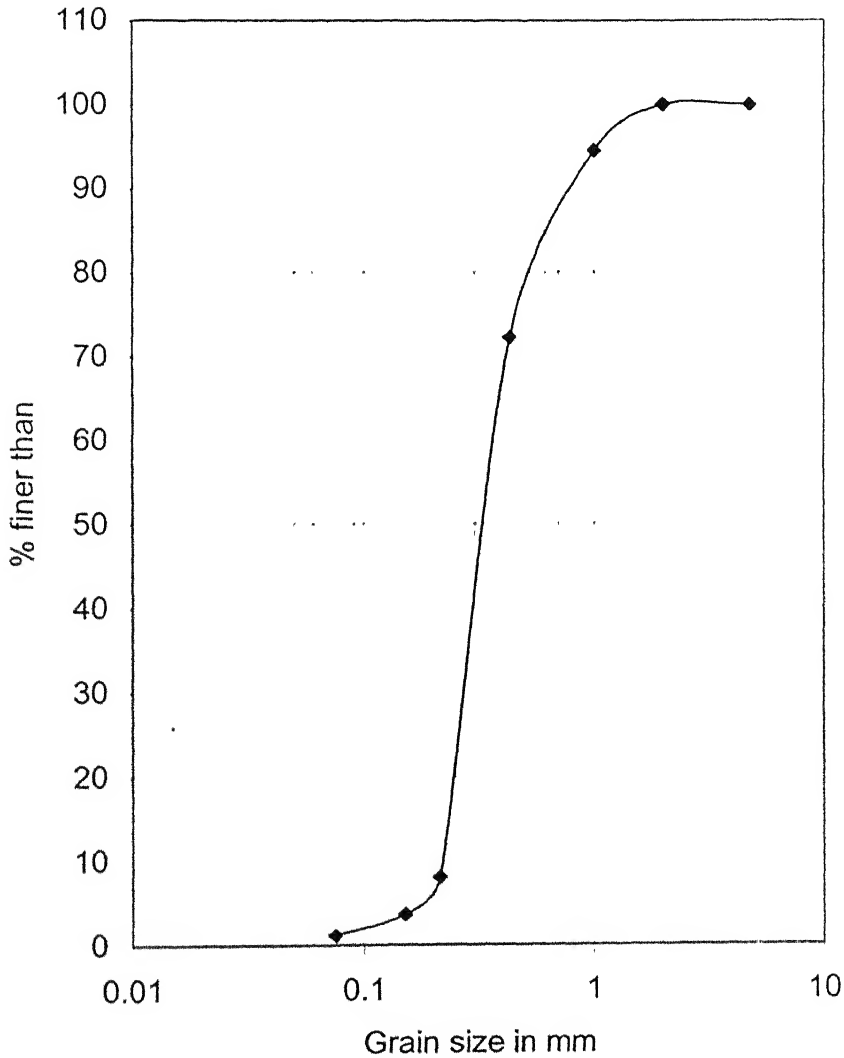

Fig. 2.2: Particle size distribution of sediment of Yamuna river sand

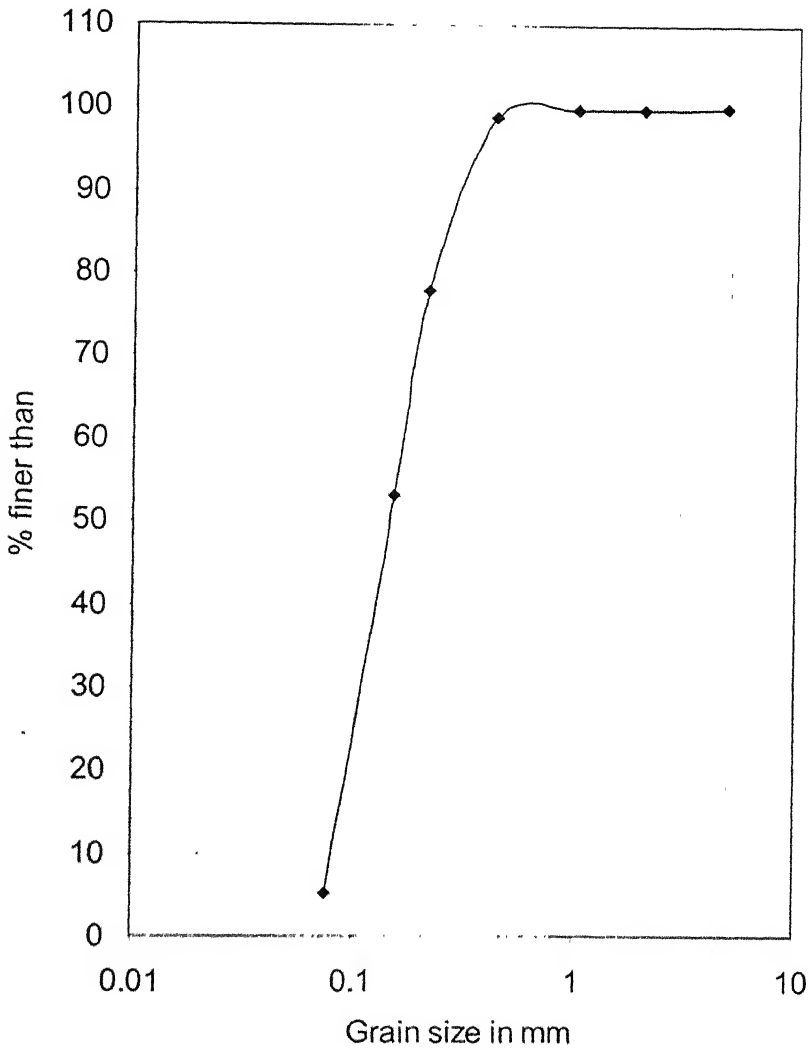

Fig.2.3: Particle size distribution of sediment of Ganga river sand

2.3 Conditions during experiments

Experiments were conducted in the channel under the following conditions:

1. Flow depth was maintained as constant throughout the duration of the experiment.
2. Flow is considered to be uniform throughout the experiments.
3. The orientation of the model in the direction of flow for all the experiments has beei so maintained that the angle of attack is taken to be 0^0.
4. The interference of walls of the channel can be neglected as the aspect ratio (B/D) i: greater than 5. Where D is the diameter of pier and B is the width of the experimenta channel.
5. Channel bed slope was negligibly small and can be considered to be horizontal.

2.4 Experimental procedure

Experiments on both the channels have the similar procedure. Before starting any experiment, sediment bed had been properly leveled and bed levels were measured along the flume length at three sections, one at the test section and the others, one at 1.0 meter upstream of the test section and last one at 1.0 meter downstream of the test section. The test section chosen was located at a distance of 3.0 meter from the inlet for Yamuna sand flume and 1.5 meter from the inlet for Ganga sand flume. Water was allowed gradually in to the channel reservoir through a valve on the upstream side of channel. After the water level builds up in the reservoir, water level is controlled by the gates provided at the inlet and outlet of the channel. The velocity of water is such that the particles move freely. The required conditions, like depth of flow and discharge were maintained steadily during each experiment. A series of experiments was conducted with piers and abutment for measuring the scour depth at the limiting equilibrium for both the channels.

Models of peirs and abutment are inserted at the test section of the channel, at different embedment depth (D, 1.5D, 1.75D, 2D, 2.5D, 3D, 3.5D and 4D). The pier was inserted at the center of the channel and abutment was inserted at the side of the wall of channel. Top of the piers and abutment was above the maximum water level. Position of piers and abutment in the channel is shown in Fig. 2.4, Fig. 2.5 and Fig. 2.6.

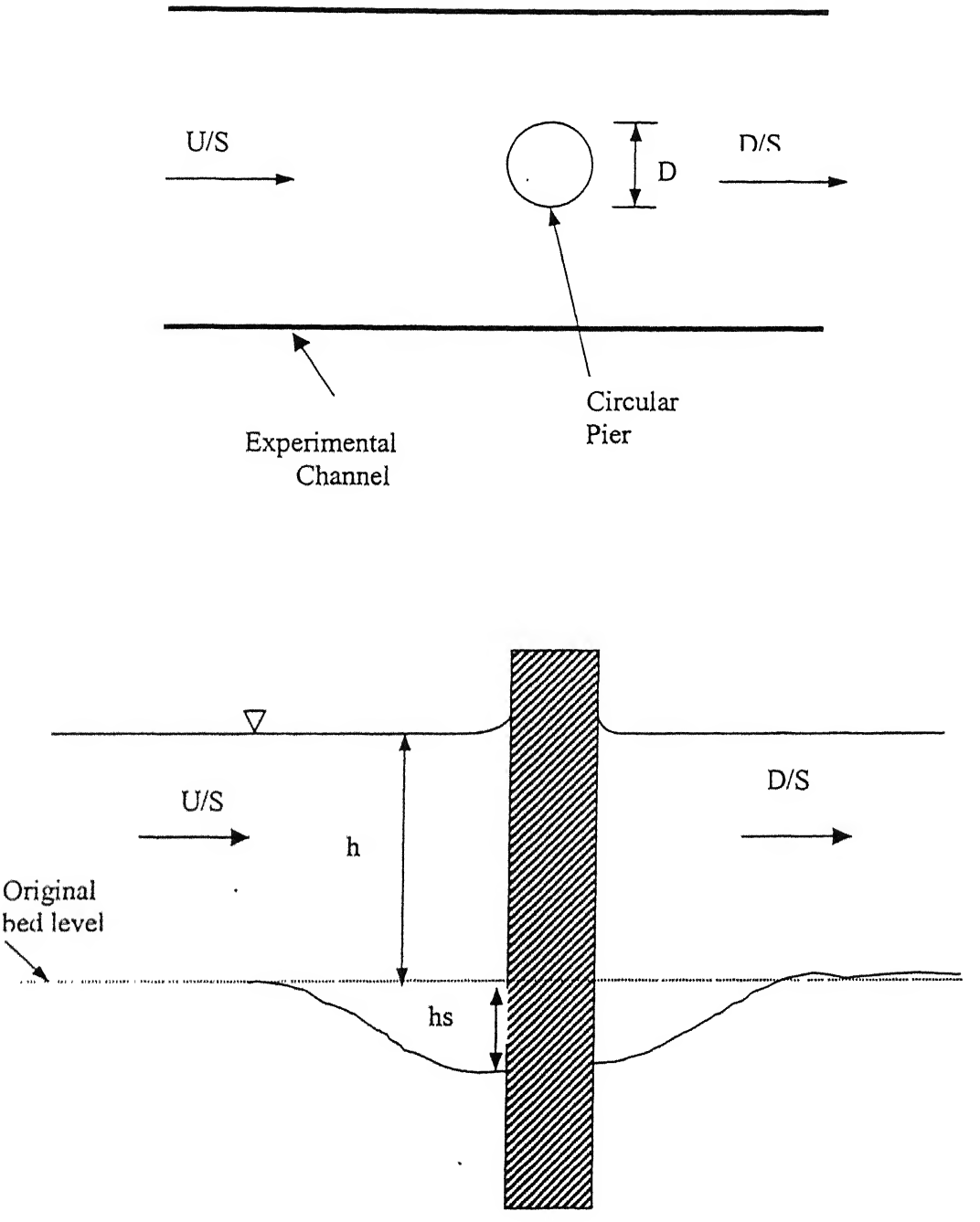

Fig. 2.4: Position of circular pier in channel

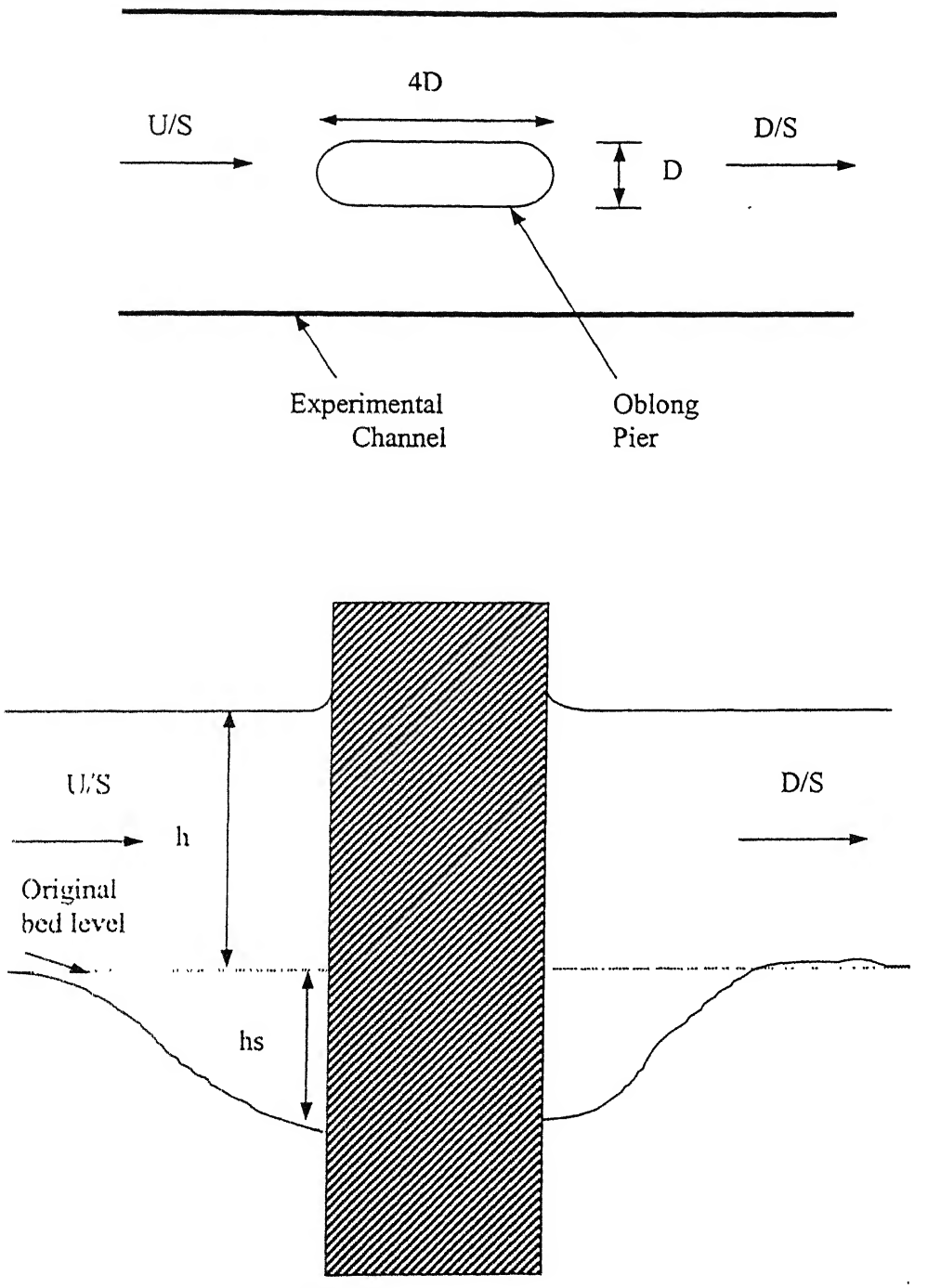

Fig. 2.5: Position of oblong pier in channel

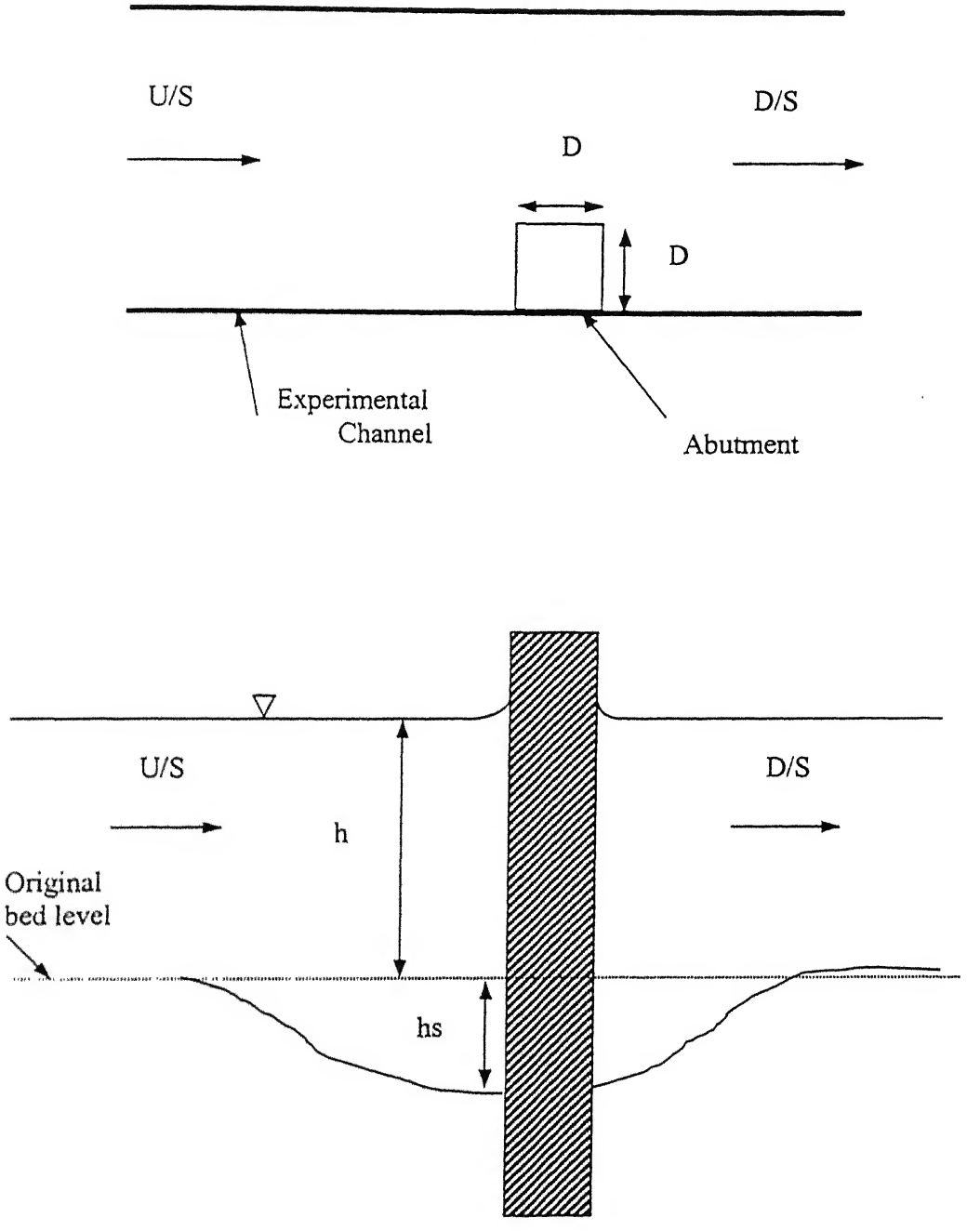

Fig. 2.6: Position of abutment in channel

2.5 Details of experiments

Cylindrical model pier made of pvc pipe with a outer diameter of 50 mm, a wooden oblong pier with semicircular ends with a width of 50 mm is used in experimental study as a model piers. A wooden square abutment with 50 mm dimensions was used as a model abutment for experimental study. Same models are used to perform experiments on fine sand and medium sand. Initial setup of pier before the start of scouring is shown in Fig. 2.7. Experiments have been conducted under varying condition of embedment depth and flow conditions. Embedment depth of piers and abutment below the sediment bed level is varied and the scour depth at which the model failed (i.e. tilted or washed away, as shown in Fig. 2.8) is measured. Flow intensity is varied with the increase of discharge and the flow depth. Flow depth is maintained between 2D to 3D. The embedment depth of models are chosen sequentially as D, 1.5D, 1.75D, 2D, 2.5D, 3D, 3.5D and 4D. Flow intensity was varied with embedment depth to cause failure of the model. After each experiment, sediment bed level was properly leveled by taking the washed sediment back to the bed from the trap, mixed well with the sand on the channel and leveled to original bed level.

2.6 Scour depth measurements

Scour depth measurements were made with the help of a point gauge with a least count of 0.1 mm. The area around the test section was illuminated with the help of a bulb, so that the observations can be made correctly. Measurements were made at the point of maximum scour around piers or abutment.

Each set of experiment was conducted for 600 minutes. Reading were taken at the following time interval namely 1, 2, 5, 7, 10, 20, 30, 50, 70, 150, 200, 300, 400, 500 and 600 minutes respectively after the initiation of scouring. Scour depth was measured at that point around pier or abutment, where the maximum scour depth occurred. After the end of each experiment sediment bed level was properly leveled. Sediments transported by water current were collected from the trap and put back in the eroded area and mixed up well with the existing sand and leveled to original bed level.

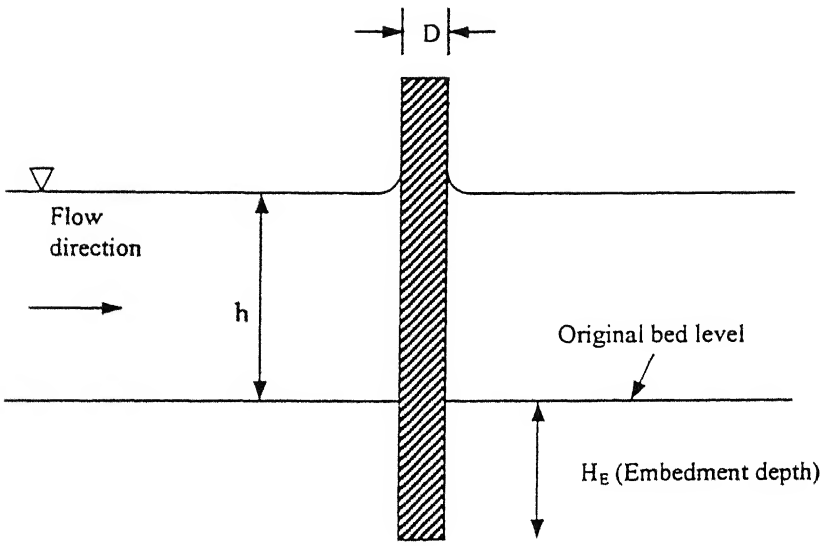

Fig. 2.7: Initial setup of pier before start of scouring

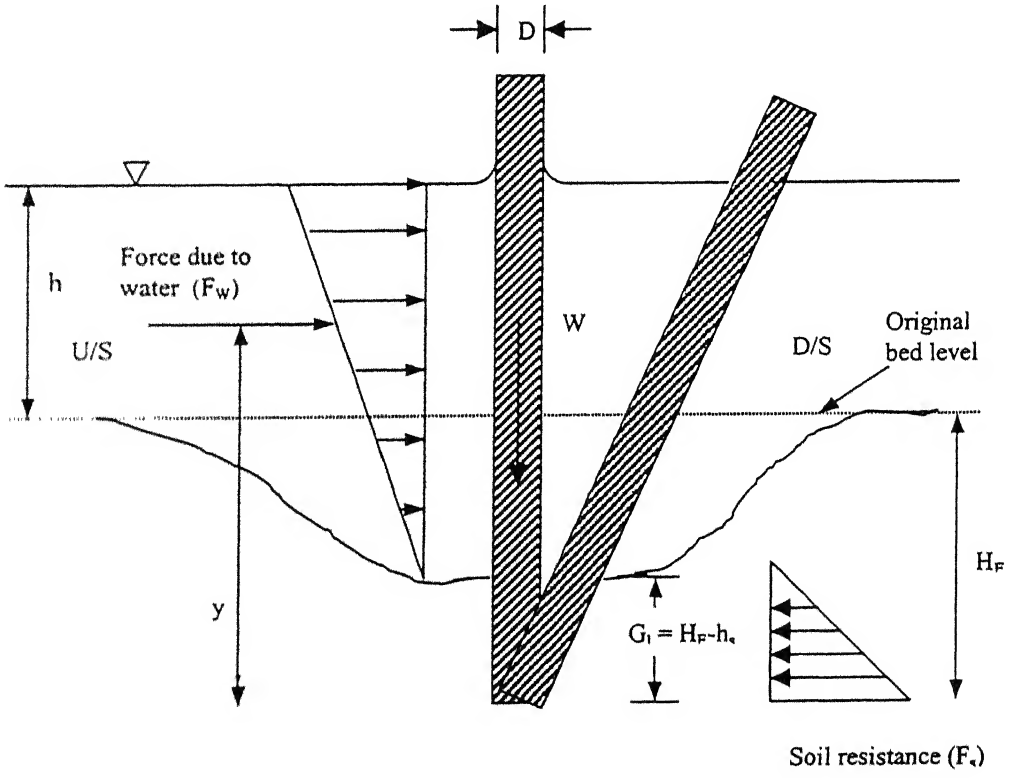

Fig. 2.8: Position of pier at the time of failure after start of scouring

CHAPTER 3

EXPERIMENTAL RESULTS AND DISCUSSION

In this chapter the data generated through various sets of experiments are presented, analyzed and discussed. Experimental observation for maximum scour depth corresponding to the limiting equilibrium for various Froude number, flow depth, embedment depth and discharge are given in Table 3.1 for Yamuna river sand and in Table 3.2 for Ganga river sand.

Scour depth (h_s) depends on depth of flow (h), diameter of pier (D), discharge intensity (q), average velocity of flow (V) and sediment silt factor (f). Based on these variables, the possible non-dimensional parameters that are considered for the analysis. They are $\frac{h_s}{h}, \frac{h}{D}, \frac{q}{\sqrt{gD^3}}, \frac{q}{\sqrt{gh^3}}$, and f. In present work an attempt has been made to develop a semi-empirical approach to predict grip length needed for piers and abutments to be stable at the limiting state (when they are just about to fail). The grip length is considered as the difference in the foundation embedment depth and scour depth, namely $G_l = H_E - h_s$. In order to study the variation of grip length G_l in terms of above flow variables h, q, and V, geometry of pier, D and sediment property in terms of silt factor 'f', regrouping of non-dimensional parameters are carried out by including, $H_E - hs$. Also, in the field and in the laboratory, the bed level goes on changing as soon as the sediment on the bed starts moving. Due to this fact scour depth is measured from free surface, even through free surface also changes with discharge intensity (q). The analysis is carried out in terms of measurements with reference to free surface. Data are also presented to find the interrelationship between flow depth, scour depth, embedment depth and pier/abutment diameter.

Figure 3.1 shows the variation of scour depth as (h+hs)/D in terms of diameter of pier with depth of foundation $(h+H_E)/D$. It can be seen from the Figure 3.2 that the above quantities bear a linear relationship with each other. An equation was formed as shown

by linear regression analysis, giving a correlation coefficient $R \approx 1$ showing excellent agreement.

Figure 3.3, shows the variation of scour depth with respect to depth of foundation as a function of depth of flow. The value $(h+h_s)/(h+H_E)$ decreases as depth of flow increases in the limited range of experiments conducted. In this case for both linear and non-linear regression analysis of the data fitting equations given in the Figure 3.4, the values obtained for correlation coefficients (0.68 and 0.70) are so close to each other that they may be considered to be same, the values being approximately 0.70 showing a good agreement.

Figure 3.5 shows the variation $(h+h_s)/(h+H_E)$ in terms of discharge intensity (q) and diameter of the pier (D) as $\frac{q}{\sqrt{gD^3}}$. The $(h+h_s)/(h+H_E)$ decreases as $\frac{q}{\sqrt{gD^3}}$ increases.

Figure 3.7, is similar to Figure 3.5. Here Froude number $\frac{q}{\sqrt{gh^3}}$ is used as the variable. The trend in the variation is similar to Figure 3.5. For both the above cases linear and power equation based on the regression analysis is shown in Figure 3.6 and 3.8 respectively. Non-linear regression analysis of the data showed better correlation than the linear regression analysis of the same. The power equation form for both the cases provided very good values for correlation coefficient ranging from 0.85 to 0.9, indicate excellent relationship between the parameters concerned.

Figure 3.9 and Figure 3.10 shows the non-dimensional value of grip length in terms of foundation depth as a function of Froude number for Yamuna sand and Ganga sand respectively. It may be seen that the Grip length required is more and more as the flow intensity in terms of Froude number increases.

Figure 3.11 and 3.12 are same as that of Figure 3.9 and 3.10, except inclusion of Lacey's silt factor 'f' in introduced along with Froude number. The variation trend is same. The values of the correlation coefficient (R) obtain from non-linear regression analysis of the data (0.85-0.94) fitting an equation in the power form show excellent correlationship between the variables.

In Figure 3.13 and 3.14, results of both sand are combined and plotted against Froude number $\left[\left\{\frac{q}{\sqrt{gh^3}}\right\}\left\{\frac{l}{f}\right\}^{\frac{1}{6}}\right]$ in Figure 3.13 and with $\frac{q}{\sqrt{gh^3}}$ in Figure 3.14. The relation is given in terms of power law. Figure 3.14 indicates better correlation between the variables can be achieved when the grip length ratio is expressed as a function of Froude number and discharge only without including the silt factor as shown in Figure 3.13. This indicates that the effect of sediment size on the variation of grip length may be not significant.

The experimental data obtained from the present study and the same by Mamgain (2001) are presented in Table 3.3 to 3.5. Non-linear regression analysis of the data is carried out to find a relationship to predict the $\left(\frac{h_s}{h}\right)$ ratio as a function of $F_R, \frac{h}{D}$, and d_{50}. Analysis is carried out by method of least square error using the STATISTICA package. The relationship obtained as follows:

$$\ln\left(\frac{h_s}{h}\right) = -1.562 - 0.45\left(\frac{h}{D}\right) + 1.15F_R^2 + 0.705d_{50}$$

For the obtained relation the coefficient of correlation is 0.76.

Similar relationship is obtained by using the silt factor instead of d_{50}. The obtained relation is as follows:

$$\ln\left(\frac{h_s}{h}\right) = -1.967 - 0.39\left(\frac{h}{D}\right) + 1.10F_R^2 + 0.647f$$

The correlation coefficient (R) for this case is 0.77 showing reasonable good fitting of equation from the data.

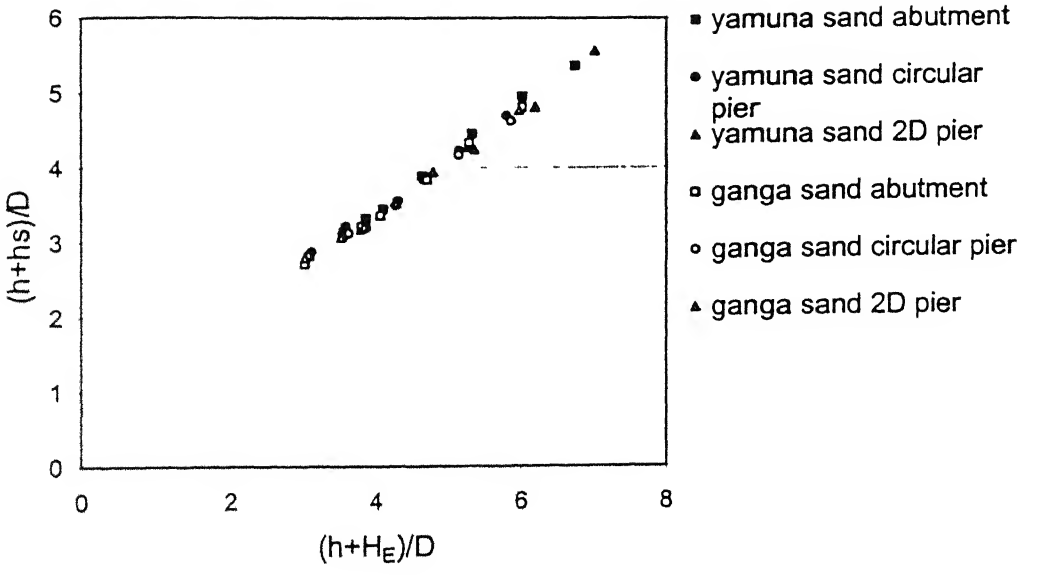

Fig. 3.1: Variation of scour depth with embedment depth

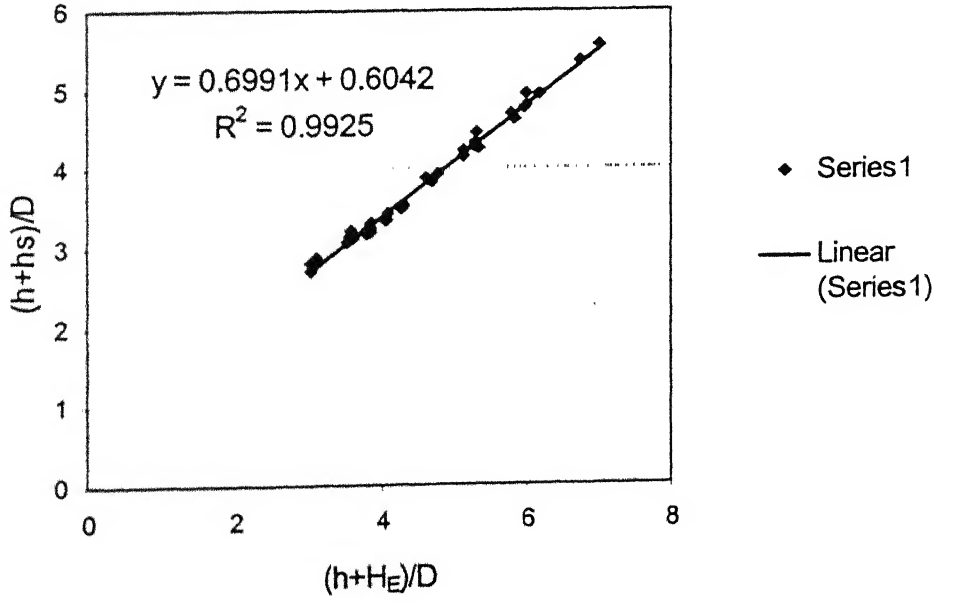

Fig. 3.2: Linear relationship between scour depth and embedment depth

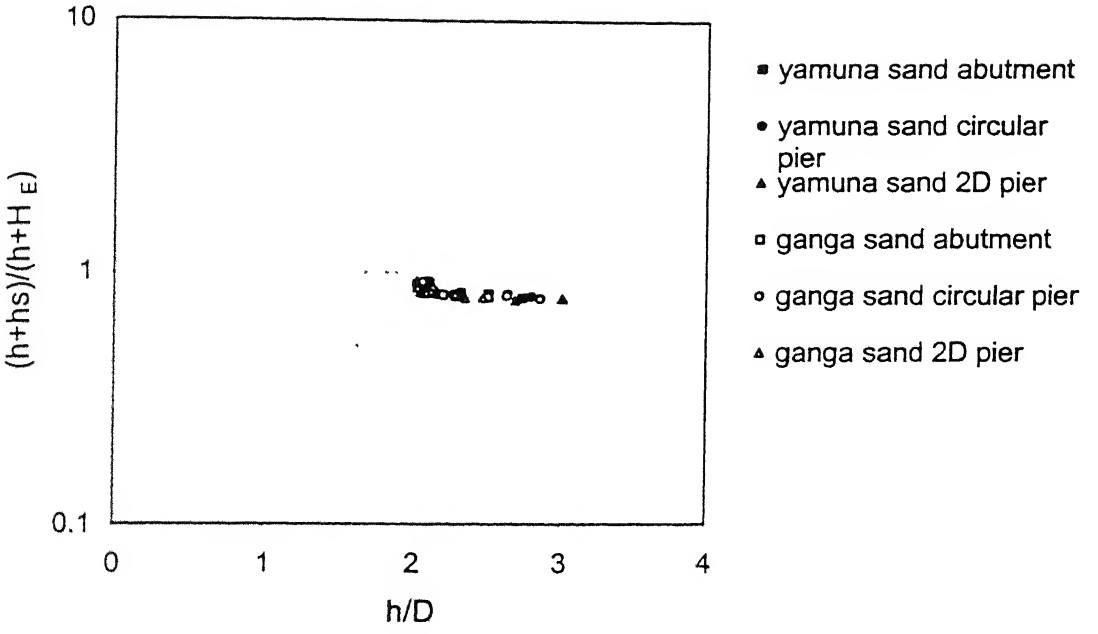

Fig. 3.3: Variation of scour depth to embedment depth ratio with flow depth ratio

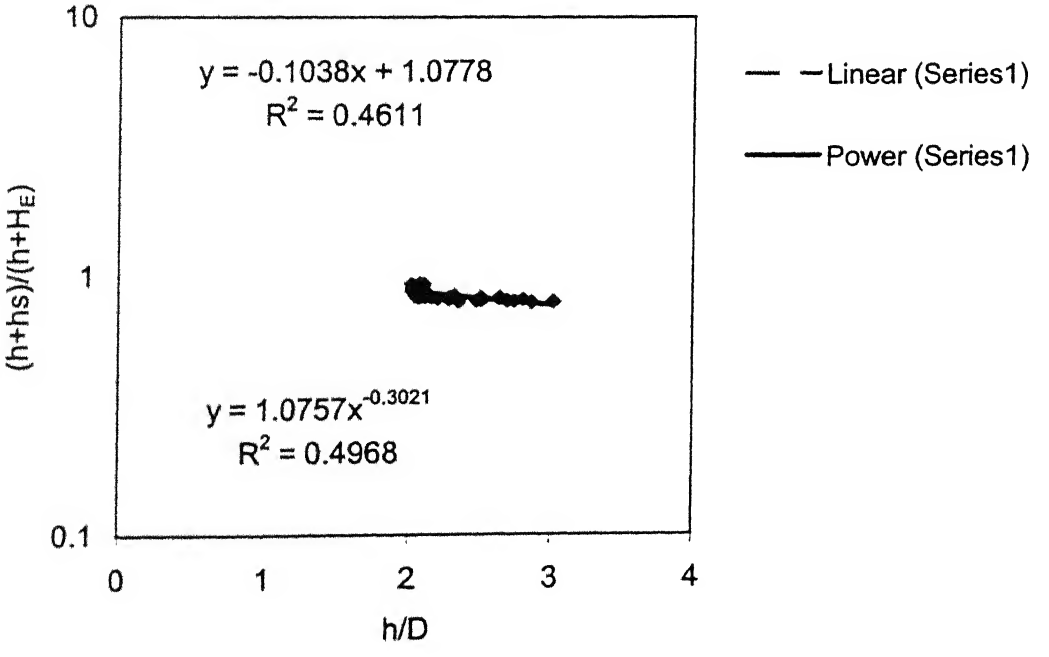

Fig. 3.4: Linear and power equations for scour depth to embedment depth ratio and flow depth ratio

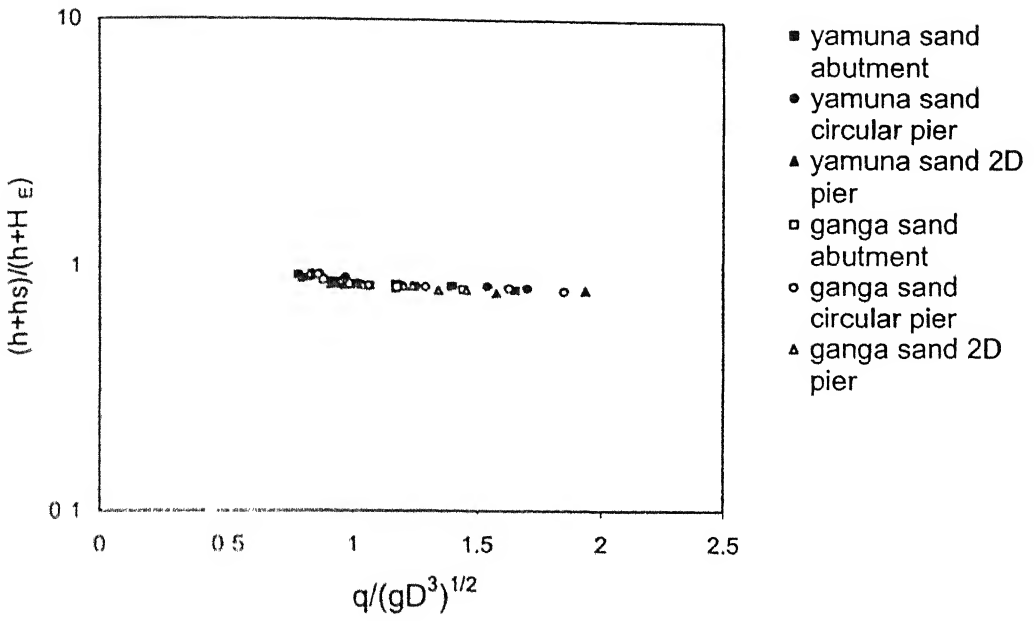

Fig.3.5: Variation of scour depth to embedment depth ratio with discharge intensity and pier diameter

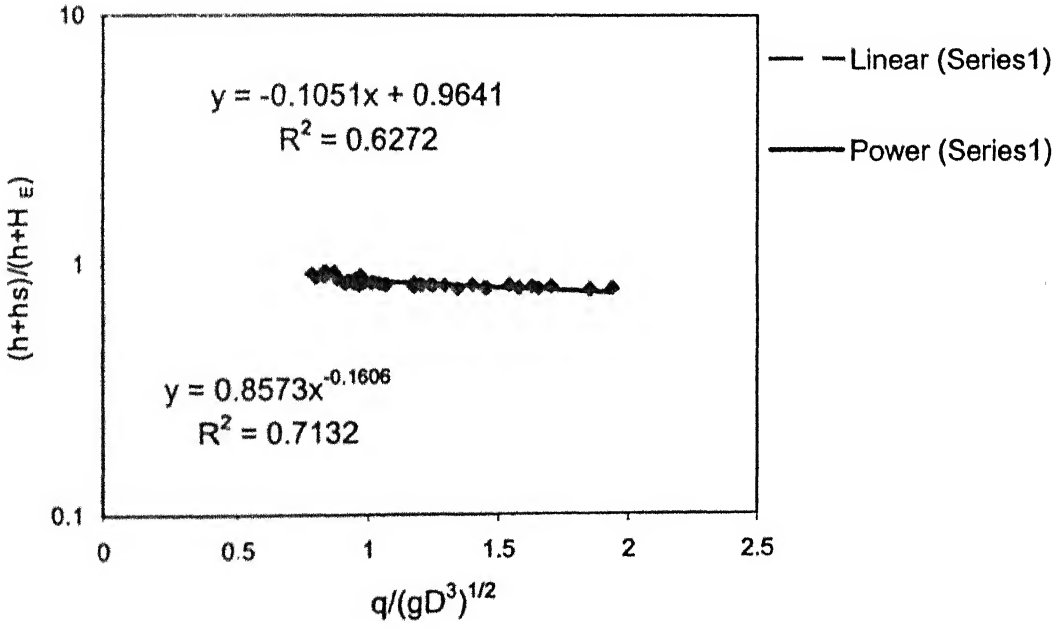

Fig.3.6: Linear and power equations for scour depth to embedment depth ratio and discharge intensity with pier diameter

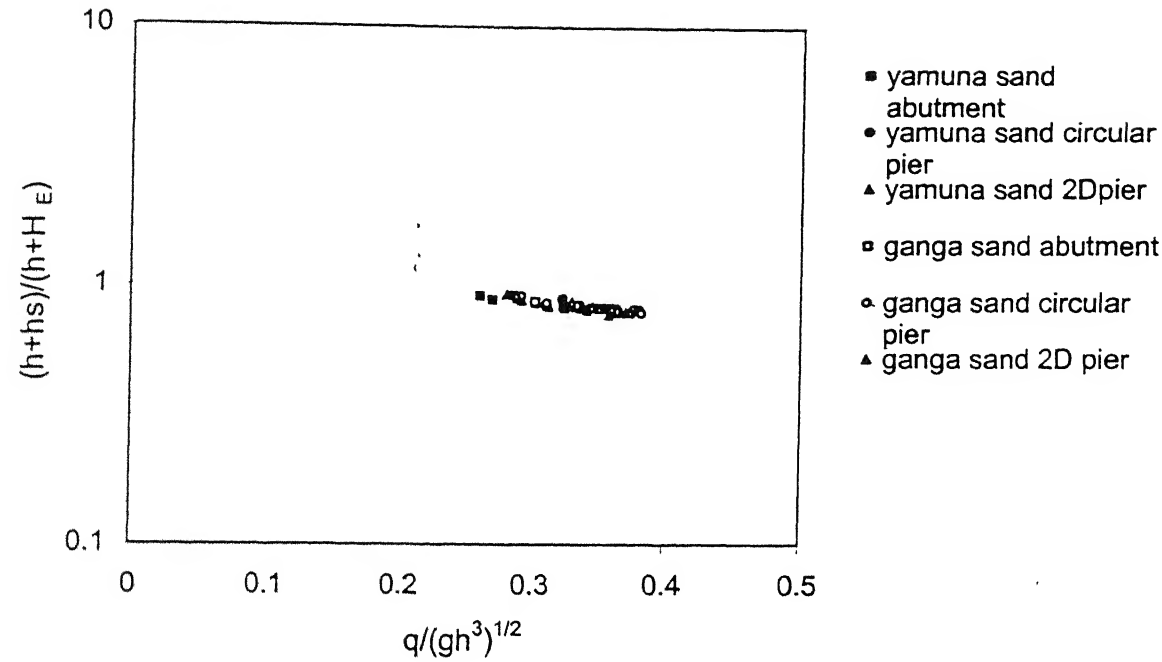

Fig.3.7: Variation of scour depth to embedment depth ratio with Froude number

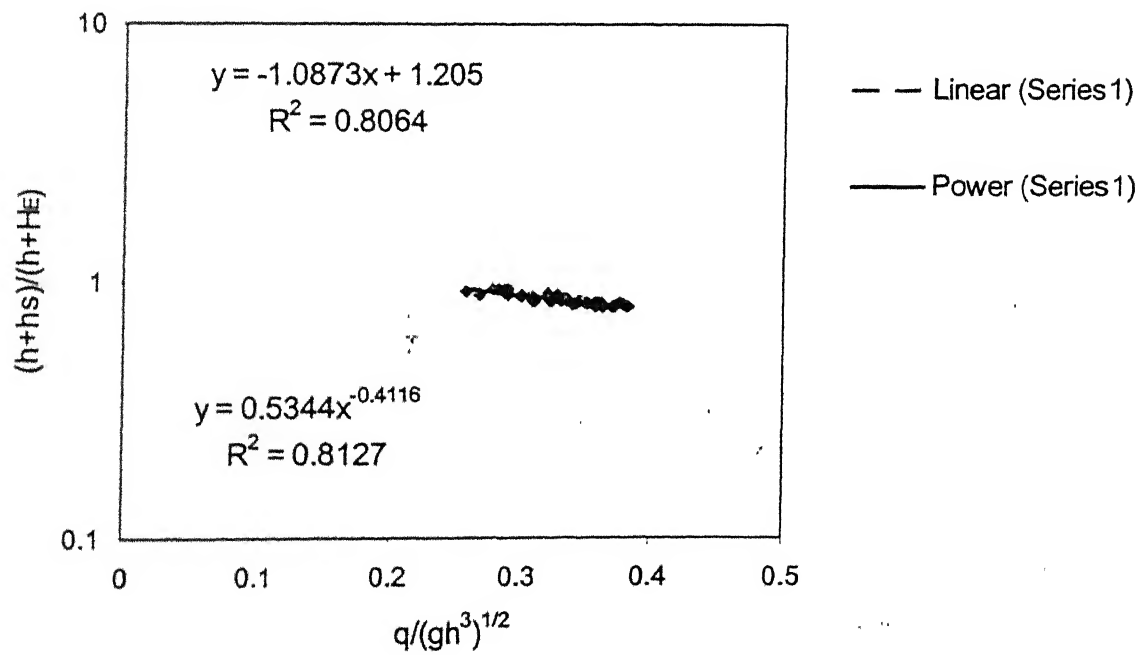

Fig.3.8 : Linear and power equations for scour depth to embedment depth ratio and Froude number

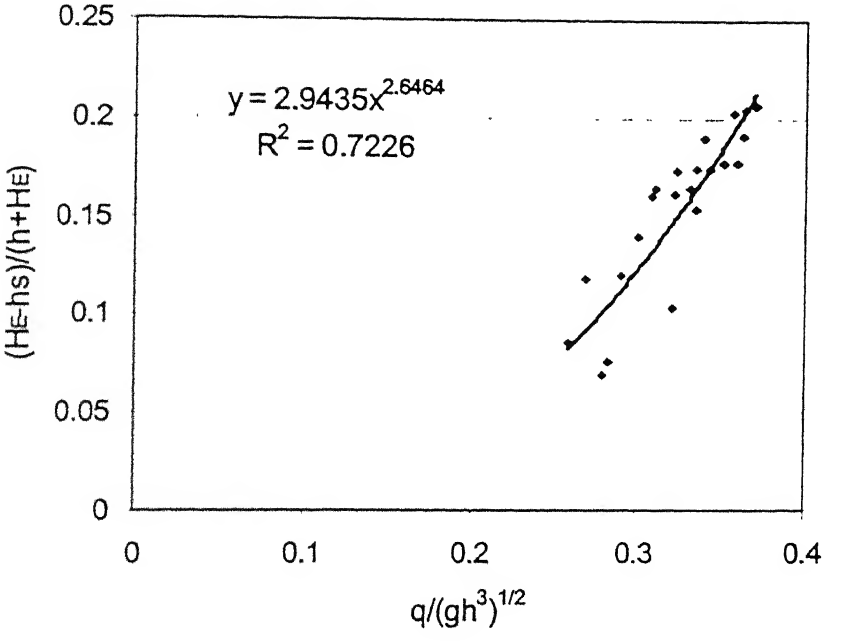

Fig.3.9: Power equation for Yamuna river sand

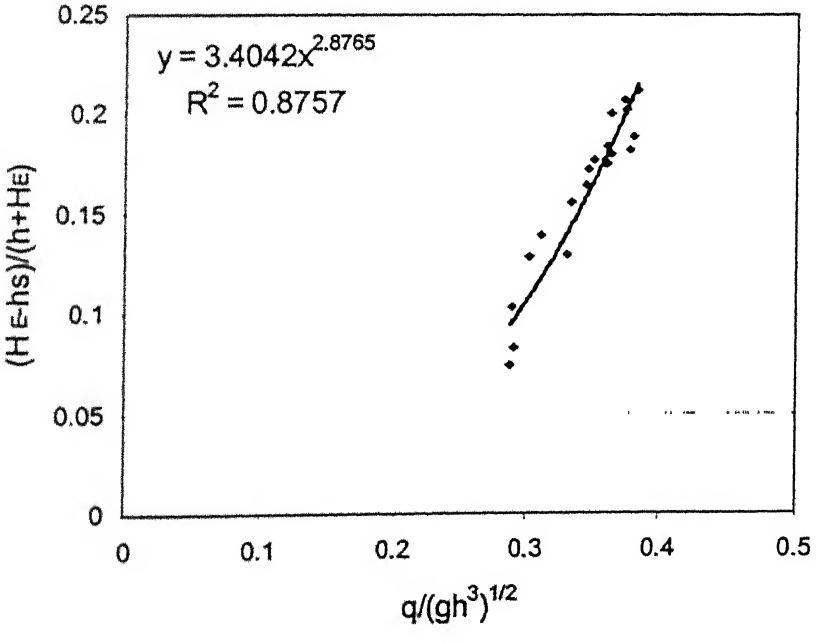

Fig.3.10: Power equation for Ganga river sand

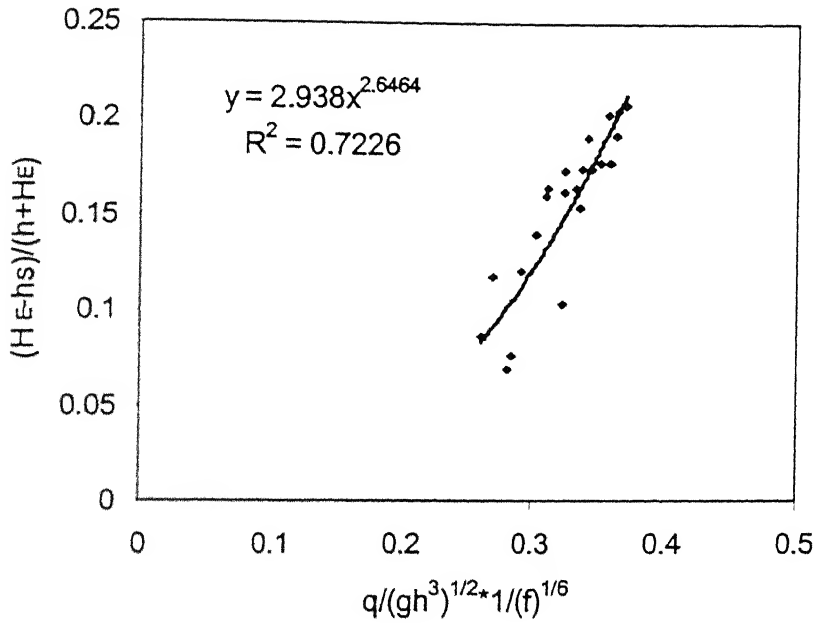

Fig. 3.11: Power equation for Yamuna river sand with silt factor

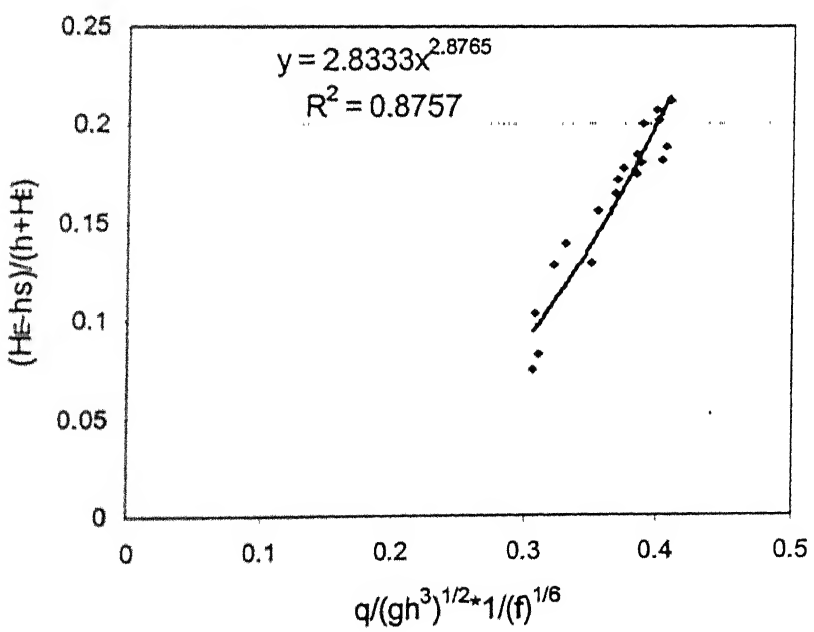

Fig.3.12: Power equation for Ganga river sand with silt factor

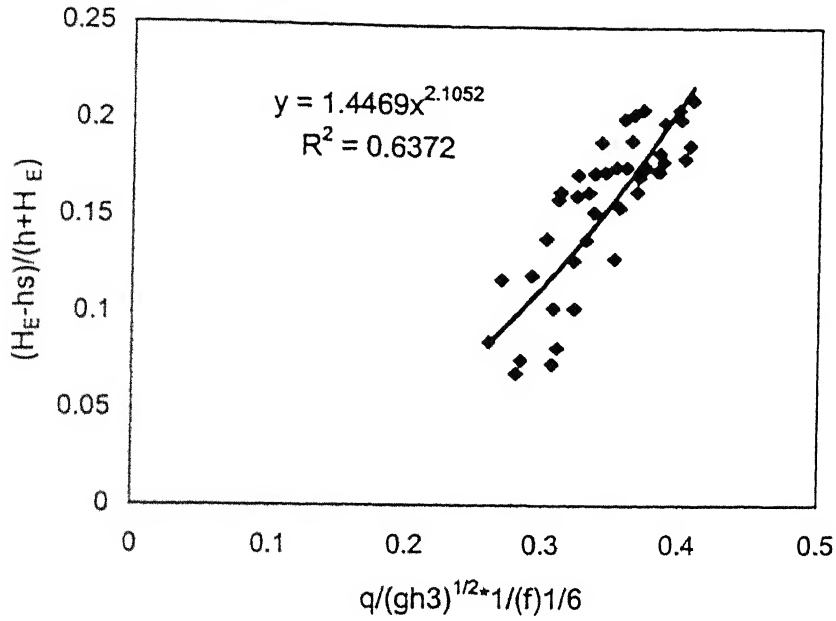

Fig. 3.13: Power equation for combined Yamuna and Ganga river sand with silt factor

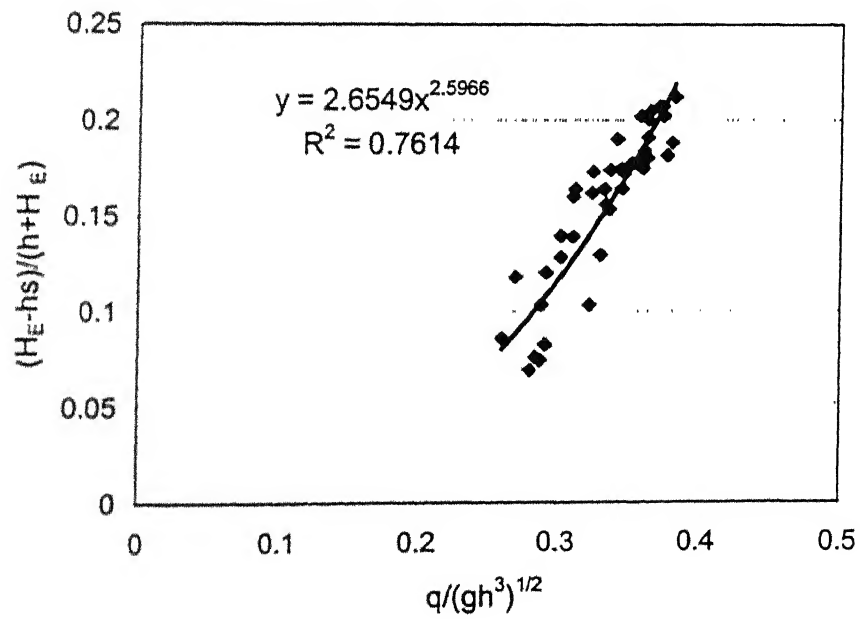

Fig. 3.14: Power equation for combined Yamuna and Ganga river sand with out silt factor

TABLE 3.1: Experimental observation for piers and abutments at failure condition for Yamuna river sand

Abutment on Yamuna sand

Embedment Depth ratio H_e/D	Flow depth Ratio h/D	Scour depth Ratio hs/D	Discharge m^3/sec/m q	Velocity m/sec V	Froude No. Fr	Experimental Observation $(G_f/h)_e$
1	2.082	0.736	0.0272	0.2622	0.2595	0.12680
1.5	2.062	1.08	0.0278	0.2705	0.2690	0.20368
1.75	2.106	1.212	0.0322	0.3063	0.3014	0.25546
2	2.098	1.344	0.0329	0.3144	0.31	0.31267
2.5	2.136	1.75	0.0353	0.3310	0.3234	0.35112
3	2.32	2.128	0.0410	0.3541	0.3320	0.37586
3.5	2.51	2.434	0.0489	0.3902	0.3517	0.42470
4	2.74	2.62	0.05781	0.4224	0.3644	0.50365

Circular pier on Yamuna sand

Embedment Depth ratio H_e/D	Flow depth Ratio h/D	Scour depth Ratio hs/D	Discharge m^3/sec/m q	Velocity m/sec V	Froude No. Fr	Experimental Observation $(G_f/h)_e$
1	2.106	0.764	0.03032	0.2879	0.3221	0.11206
1.5	2.084	1.13	0.03394	0.3257	0.3358	0.17754
1.75	2.094	1.16	0.03564	0.3404	0.3437	0.28175
2	2.3	1.25	0.041986	0.3650	0.3593	0.32608
2.5	2.64	1.59	0.05398	0.4089	0.3630	0.34469
3	2.8	1.892	0.05956	0.4254	0.3797	0.39571

Oblong pier on Yamuna sand

Embedment Depth ratio H_e/D	Flow depth Ratio h/D	Scour depth Ratio hs/D	Discharge m^3/sec/m q	Velocity m/sec V	Froude No. Fr	Experimental Observation $(G_f/h)_e$
1	2.076	0.788	0.02930	0.2823	0.2797	0.1021
1.5	2.094	1.068	0.03088	0.2950	0.2911	0.2063
1.75	2.044	1.128	0.03185	0.3117	0.3113	0.3043
2	2.07	1.296	0.03377	0.3263	0.3238	0.3400
2.5	2.16	1.69	0.03739	0.3462	0.3363	0.375
3	2.28	1.996	0.04108	0.3604	0.3408	0.4403
3.5	2.69	2.248	0.05524	0.4107	0.3575	0.4654
4	3.01	2.548	0.06778	0.4504	0.3707	0.4823

TABLE 3.2: Experimental observation for piers and abutments at failure condition for Ganga river sand

Abutment on Ganga sand

Embedment Depth ratio H_E/D	Flow depth Ratio h/D	Scour depth Ratio hs/D	Discharge $m^3/sec/m$ q	Velocity m/sec V	Froude No. Fr	Experimental Observation $(G_f/h)_e$
1	2.024	0.688	0.02904	0.2869	0.288	0.1541
1.5	2.04	1.046	0.03075	0.3015	0.3014	0.2225
1.75	2.056	1.156	0.03438	0.3344	0.3330	0.2889
2	2.066	1.288	0.03729	0.3610	0.3586	0.3446
2.5	2.2	1.634	0.04119	0.3744	0.3604	0.3936
3	2.28	2.048	0.04371	0.3835	0.3626	0.4175
3.5	2.51	2.296	0.05059	0.4031	0.3632	0.4796

Circular pier on Ganga sand

Embedment Depth ratio H_E/D	Flow depth Ratio h/D	Scour depth Ratio hs/D	Discharge $m^3/sec/m$ q	Velocity m/sec V	Froude No. Fr	Experimental Observation $(G_f/h)_e$
1	2.06	0.748	0.03009	0.2921	0.2906	0.1223
1.5	2.126	0.996	0.03367	0.3167	0.3101	0.2370
1.75	2.11	1.086	0.03715	0.3521	0.3462	0.3146
2	2.272	1.224	0.04521	0.3980	0.3770	0.3415
2.5	2.636	1.532	0.05702	0.4326	0.3804	0.3672
3	2.86	1.756	0.06478	0.4530	0.3825	0.4349

Oblong pier on Ganag sand

Embedment Depth ratio H_E/D	Flow depth Ratio h/D	Scour depth Ratio hs/D	Discharge $m^3/sec/m$ q	Velocity m/sec V	Froude No. Fr	Experimental Observation $(G_f/h)_e$
1	2.02	0.776	0.02888	0.2859	0.2873	0.1108
1.5	2.024	1.044	0.03322	0.3283	0.3295	0.2252
1.75	2.086	1.12	0.03639	0.3489	0.3449	0.3020
2	2.278	1.242	0.04218	0.3703	0.3503	0.3327
2.5	2.28	1.664	0.0434	0.3807	0.36	0.3666
3	2.35	1.892	0.04704	0.4004	0.3729	0.4714
3.5	2.474	2.292	0.05097	0.4121	0.3741	0.4882

Table 3.3: Present data of Yamuna river sand with 0.32 mm medium size (d_{50})

Scour depth/Flow depth (h_s/h)	Flow depth ratio (h/D)	Froude number (F_R)
0.3535	2.082	0.2595
0.5237	2.062	0.269
0.5754	2.106	0.3014
0.6406	2.098	0.31
0.8192	2.136	0.3233
0.9172	2.32	0.3320
0.9697	2.51	0.3517
0.9562	2.74	0.3644
0.3627	2.106	0.2833
0.5422	2.084	0.3221
0.5539	2.094	0.3358
0.5434	2.3	0.3437
0.6022	2.64	0.3593
0.6757	2.8	0.3630
0.3795	2.076	0.2797
0.5100	2.094	0.2911
0.5518	2.044	0.3113
0.6260	2.07	0.3238
0.7824	2.16	0.3363
0.8754	2.28	0.3408
0.8356	2.69	0.3575
0.8465	3.01	0.3707

Table 3.4: Present data of Ganga river sand with 0.15 mm medium size (d_{50})

Scour depth/Flow depth (h_s/h)	Flow depth ratio (h/D)	Froude number (F_R)
0.3399	2.024	0.288
0.5127	2.04	0.3014
0.5622	2.056	0.3330
0.6234	2.066	0.3586
0.7427	2.2	0.3604
0.8982	2.28	0.3626
0.9147	2.51	0.3632
0.3631	2.06	0.2906
0.4684	2.126	0.3101
0.5146	2.11	0.3462
0.5387	2.272	0.3770
0.5811	2.636	0.3804
0.6139	2.86	0.3825
0.3841	2.02	0.2873
0.5158	2.024	0.3295
0.5369	2.086	0.3449
0.5452	2.278	0.3503
0.7298	2.28	0.36
0.8051	2.35	0.3729
0.9264	2.474	0.3741

Table 3.5: Mamgain (2001) data of Yamuna river sand with 0.60 mm medium size (d_{50})

Scour depth/Flow depth (h_s/h)	Flow depth ratio (h/D)	Froude number (F_R)
0.4604	2.471	0.2330
0.4860	2.633	0.2483
0.4747	2.688	0.2534
0.4481	2.99	0.2819
0.4473	3.174	0.3174
0.4910	3.329	0.3139
0.5457	3.382	0.3189

CHAPTER 4

THEREOTICAL PREDICTION AND COMPARISION WITH EXPERIMENTAL DATA

4.1 General

Embedment depth of piers and abutments below the bed sediment bed level is an important factor for the stability of structure against failure due to overturning caused by the horizontal and lateral forces. Adequate embedment depth imparts resistance against these forces due to wind, water and earthquake etc.

Flow conditions in rivers may vary due to flood. Flood flow develops a horseshoe vortex at the front junction corner of piers or abutments with sediment bed. The scouring action of this horseshoe vortex lead to the significant scouring around bridge piers and abutments situated in rivers. Because of scouring, considerable length of piers and abutment is exposed due to erosion of soil on upstream face of the piers and abutments facing flow. This reduces the grip length of piers and abutments, leading to instability of structure.

Experiments were conducted with different flow conditions, i.e. varying the discharge with the variation of embedment depth below the bed level on two different sediment sizes in the bed. The aim is to predict the grip length just safe against failure of structures like piers and abutments. Maximum scour depth measured at the point of model failure (tilted or washed away).

4.2 Theoretical predictive model

A theoretical model based on the equilibrium of forces acting on the model has been developed to predict the limiting value of the scour depth at the point of incipient failure. The assumptions made are as follows:

1) Force due to flowing water acting on the pier and abutment is assumed to be in a triangular pattern i.e. maximum at the water level and zero at the maximum scouring level

2) Weight of the pier and abutment and load acting over the structure are neglected.

3) Flow condition is assumed to be uniform through out the experiments.

4) Interference of the walls of the channel is neglected.

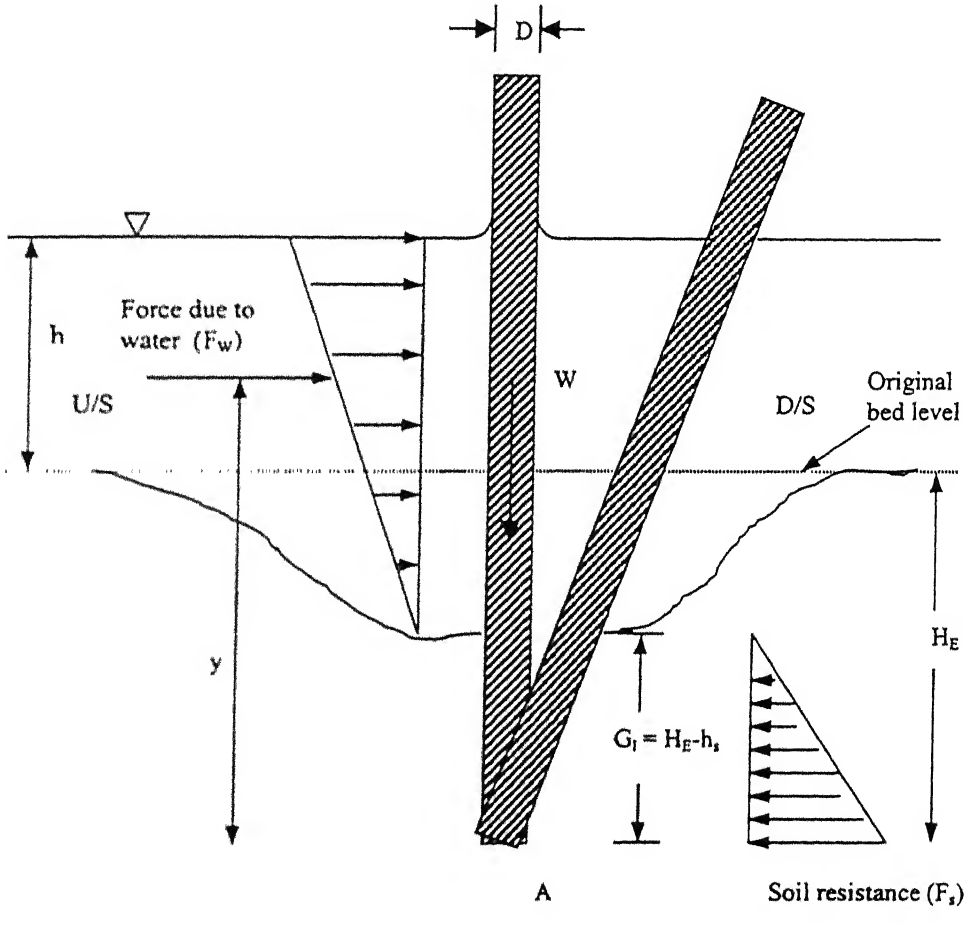

Fig. 4.1: Definition sketch

4.2.1 Derivation

Notations used in the analysis, with reference to fig. 4.1, the different symbols signify the following:

w_1 = Weight of the super structure

w_s = Weight of the pier

W = Weight of superstructure + Weight of peir

h = Flow depth

h_s = Scour depth

U = Mean velocity of flow

D = Diameter of pier

γ'_s = Submerged density of soil

H_E = Embedment depth of pier below the sediment bed level

y = Distance from foundation base at which the force due to water current acts

G_1 = Grip length = $H_E - h_s$

C_D = Drag coefficient

F_R = Modified Froud number

K_p = Coefficient of passive earth pressure

d_{50} = size for which 50% of the sediment by weight is finer

(a) Force due to water current:

$$F_W = \tfrac{1}{2}[(1/2)\rho C_D U^2 D (h + h_s)] \quad (4.1)$$

This force is acting from foundation base A at a distance

$$y = [(H_E - h_s) + 2/3 (h + h_s)]$$

(b) Soil resisting force:

Soil resistance F_s is estimated by using Broms's approach (1964) as follows:

$$F_s = \frac{1}{2} \times 3\gamma'_s D G_1 K_p . G_1 \quad (4.2)$$

$$= \frac{3}{2}\gamma'_s D G_1^2 K_p$$

$$= \frac{3}{2}\rho'_s g K_p D (H_E - h_s)^2$$

This force act at a distance of $\left[\frac{G_1}{3}=\frac{1}{3}(H_E-h_s)\right]$ from the foundation base.

Taking moment of all the forces about the foundation base of pier at point A

$$F_W\times\left[(H_E-h_s)+\frac{2}{3}(h+h_s)\right]=F_s\times\frac{1}{3}(H_E-h_s)+(w_l+w_s)\frac{D}{2}$$

Putting the value of F_w and F_s

$$\frac{1}{2}\left[\frac{1}{2}\rho C_D U^2 D(h+h_s)\right]\left[(H_E-h_s)+\frac{2}{3}(h+h_s)\right]$$
$$=\frac{3}{2}\rho_s' g D K_p (H_E-h_s)^2\frac{1}{3}(H_E-h_s)+(w_l+w_s)\frac{D}{2}$$

on simplifying, we get:

$$\frac{\rho C_D U^2}{2\rho_s' g K_p}=\frac{\left[(H_E-h_s)^3+\frac{(w_1+w_s)}{\rho_s' g K_p}\right]}{(h+h_s)\left[(H_E-h_s)+\frac{2}{3}(h+h_s)\right]}$$

$$\text{Let } F_R^2=\frac{\left[\left(\frac{H_E-h_s}{h}\right)^3+\frac{(w_1+w_s)}{\rho_s' g K_p h^3}\right]}{\left(1+\frac{h_s}{h}\right)\left[\left(\frac{H_E-h_s}{h}\right)+\frac{2}{3}\left(1+\frac{h_s}{h}\right)\right]}$$

Since Grip length $(G_1)=(H_E-h_s)$

$$F_R^2=\frac{\left[\left(\frac{G_1}{h}\right)^3+\frac{(w_1+w_s)}{\rho_s' g K_p h^3}\right]}{\left(1+\frac{h_s}{h}\right)\left[\left(\frac{G_1}{h}\right)+\frac{2}{3}\left(1+\frac{hs}{h}\right)\right]}$$

$$\frac{2}{3}\left(1+\frac{h_s}{h}\right)^2 F_R^2+F_R^2\left(1+\frac{h_s}{h}\right)\left(\frac{G_1}{h}\right)-\left[\left(\frac{G_1}{h}\right)^3+\frac{(w_1+w_s)}{\rho_s' g K_p h^3}\right]=0 \qquad (4.3)$$

Solving the above equation, we get

$$\left(1+\frac{h_s}{h}\right)=\frac{3}{4}\left[-\left(\frac{G_1}{h}\right)\pm\sqrt{\left\{\left(\frac{G_1}{h}\right)^2+\frac{8}{3}\frac{1}{F_R^2}\left(\left(\frac{G_1}{h}\right)^3+\frac{(w_1+w_s)}{\rho_s' g K_p h^3}\right)\right\}}\right]$$

Neglecting the weight of pier and superstructure; i.e. w_1 & $w_s \approx 0$, and taking +ve sign:

$$\left(1+\frac{h_s}{h}\right)=\frac{3}{4}\left[-\left(\frac{G_1}{h}\right)+\sqrt{\left\{\left(\frac{G_1}{h}\right)^2+\frac{8}{3}\frac{1}{F_R^2}\left(\frac{G_1}{h}\right)^3\right\}}\right] \tag{4.4}$$

In the above expression the equation obtained by carrying out non-linear regression analysis of the data obtained from experimental observations is replaced. Two model are fitted as follows:

Model 1:

From the experimental observations, the following relationship between $\frac{h_s}{h}, F_R^2, \frac{h}{D}$, and d_{50} has been obtained:

$$\ln\left(\frac{h_s}{h}\right)=-1.562-0.45\left(\frac{h}{D}\right)+1.15F_R^2+0.705d_{50} \tag{4.5}$$

Substituting the value of $\frac{h_s}{h}$ in equation (4.4):

$$\left[1+\exp\left\{-1.562-0.45\left(\frac{h}{D}\right)+1.15F_R^2+0.705d_{50}\right\}\right]=\frac{3}{4}\left[-\left(\frac{G_1}{h}\right)+\sqrt{\left\{\left(\frac{G_1}{h}\right)^2+\frac{8}{3}\frac{1}{F_R^2}\left(\frac{G_1}{h}\right)^3\right\}}\right] \tag{4.6}$$

Let:

$$a=\frac{4}{3}\left[1+\exp\left\{-1.562-0.45\left(\frac{h}{D}\right)+1.15F_R^2+0.705d_{50}\right\}\right],$$

$$b=\frac{8}{3}\frac{1}{F_R^2}$$

and $\frac{G_1}{h}=x$

now equation (4.6) can be written as:

$$a = \left| -x + \sqrt{(x^2 + bx^3)} \right|$$

$$1 + \frac{a}{x} = \sqrt{(1 + bx)}$$

squaring and simplifying the above equation:

$$x^3 + \left(-\frac{2a}{b} \right) x + \left(-\frac{a^2}{b} \right) = 0 \qquad (4.7)$$

which is in the form of polynomial of third degree. Solving the above equation we get the roots of the above equation, which corresponds to the theoretically predicted values of $\frac{G_l}{h}$.

Model 2:

Similarly as describe in chapter 3, from the experimental observations, the following relationship between $\frac{h_s}{h}, F_R^2, \frac{h}{D}$, and Lacey's silt factor f has been obtained:

$$\ln\left(\frac{h_s}{h}\right) = -1.967 - 0.39\left(\frac{h}{D}\right) + 1.10F_R^2 + 0.647f \qquad (4.8)$$

Substituting the value of $\frac{h_s}{h}$ in equation (4.4):

$$\left[1 + \exp\left\{-1.967 - 0.39\left(\frac{h}{D}\right) + 1.10F_R^2 + 0.647f\right\}\right] = \frac{3}{4}\left[-\left(\frac{G_l}{h}\right) + \sqrt{\left\{\left(\frac{G_l}{h}\right)^2 + \frac{8}{3}\frac{1}{F_R^2}\left(\frac{G_l}{h}\right)^3\right\}}\right] \qquad (4.9)$$

Let:

$$a = \frac{4}{3}\left[1 + \exp\left\{-1.967 - 0.39\left(\frac{h}{D}\right) + 1.10F_R^2 + 0.647f\right\}\right],$$

$$b = \frac{8}{3}\frac{1}{F_R^2}$$

and $\frac{G_l}{h} = x$

now equation (4.9) can be written as:

$$a = \left| -x + \sqrt{(x^2 + bx^3)} \right|$$

$$1 + \frac{a}{x} = \sqrt{(1 + bx)}$$

squaring and simplifying the above equation:

$$x^3 + \left(-\frac{2a}{b}\right)x + \left(-\frac{a^2}{b}\right) = 0 \qquad (4.10)$$

which is in the form of polynomial of third degree. Solving the above equation we get the roots of the above equation, which corresponds to the theoretically predicted values of $\frac{G_l}{h}$.

The theoretical predicted values of $\left(\frac{G_l}{h}\right)$ ratio from the suggested equation are presented along with the experimental value. To demonstrate the accuracy of the predicted values, values of Goodness ratio defined as the ratio of the theoretically predicted values of $\left(\frac{G_l}{h}\right)$ ratio to that obtained from the experimental observation, are estimated and presented in Table 4.2.1.1 to Table 4.2.1.3 for Yamuna sand and Table 4.2.1.4 to Table 4.2.1.6 for Ganga sand, for model 1. The same for model 2 is presented in Table 4.2.2.1 to Table 4.2.2.3 and Table 4.2.2.4 to Table 4.2.2.6 for Yamuna and Ganga river sand respectively. Mamgain (2001) data for Yamuna sand are given in Table 4.2.1.7 and Table 4.2.2.7 for model 1 and model 2 respectively.

It can be seen from these tables that for $\frac{H_E}{D}$ ratio greater than 2 the prediction are reasonable good as indicated by the Goodness ratio ranging with 1.13 to 1.67

TABLE 4.2.1: Experimental observations and theoretical prediction for model 1

Table 4.2.1.1: Abutment on Yamuna sand

Sl. No.	Embedment Depth Ratio H_E/D	Flow Depth Ratio h/D	Scour Depth Ratio hs/D	Discharge m^3/Sec/m	Velocity (m/sec) V	Froude No. F_R	Experimental Observations $(G_f/h)_e$	Theoretical Prediction $(G_f/h)_t$	Goodness Ratio $\frac{(G_f/h)_t}{(G_f/h)_e}$
1	1	2.082	0.736	0.0272	0.2622	0.2595	0.12680	0.4452	3.51
2	1.5	2.062	1.08	0.0278	0.2705	0.2690	0.20368	0.458	2.25
3	1.75	2.106	1.212	0.0322	0.3063	0.3014	0.25546	0.4996	1.95
4	2	2.098	1.344	0.0329	0.3144	0.31	0.31267	0.5108	1.63
5	2.5	2.136	1.75	0.0353	0.3310	0.3234	0.35112	0.5274	1.50
6	3	2.32	2.128	0.0410	0.3541	0.3320	0.37586	0.5358	1.42
6	3.5	2.51	2.434	0.0489	0.3902	0.3517	0.42470	0.5581	1.31
8	4	2.74	2.62	0.05781	0.4224	0.3644	0.50365	0.571	1.13

Table 4.2.1.2: Circular pier on Yamuna sand

Sl. No.	Embedment Depth Ratio H_E/D	Flow Depth Ratio h/D	Scour Depth Ratio hs/D	Discharge m^3/Sec/m	Velocity (m/sec) V	Froude No. F_R	Experimental Observations $(G_f/h)_e$	Theoretical Prediction $(G_f/h)_t$	Goodness Ratio $\frac{(G_f/h)_t}{(G_f/h)_e}$
1	1	2.106	0.764	0.03032	0.2879	0.2833	0.11206	0.4761	4.25
2	1.5	2.084	1.13	0.03394	0.3257	0.3221	0.17754	0.5266	2.96
3	1.75	2.094	1.16	0.03564	0.3404	0.3358	0.28175	0.544	1.93
4	2	2.3	1.25	0.041986	0.3650	0.3437	0.32608	0.5509	1.69
5	2.5	2.64	1.59	0.05398	0.4089	0.3593	0.34469	0.566	1.64
6	3	2.8	1.892	0.05956	0.4254	0.3630	0.39571	0.5685	1.43

Table 4.2.1.3: Oblong pier on Yamuna sand

Sl. No.	Embedment Depth Ratio H_E/D	Flow Depth Ratio h/D	Scour Depth Ratio hs/D	Discharge m^3/Sec/m	Velocity (m/sec) V	Froude No. F_R	Experimental Observations $(G_f/h)_e$	Theoretical Prediction $(G_f/h)_t$	Goodness Ratio $\frac{(G_f/h)_t}{(G_f/h)_e}$
1	1	2.076	0.788	0.02930	0.2823	0.2797	0.1021	0.4719	4.62
2	1.5	2.094	1.068	0.03088	0.2950	0.2911	0.2063	0.4864	2.35
3	1.75	2.044	1.128	0.03185	0.3117	0.3113	0.3043	0.5133	1.68
4	2	2.07	1.296	0.03377	0.3263	0.3238	0.3400	0.529	1.55
5	2.5	2.16	1.69	0.03739	0.3462	0.3363	0.375	0.5436	1.45
6	3	2.28	1.996	0.04108	0.3604	0.3408	0.4403	0.5475	1.24
7	3.5	2.69	2.248	0.05524	0.4107	0.3575	0.4654	0.5631	1.21
8	4	3.01	2.548	0.06778	0.4504	0.3707	0.48239	0.5756	1.19

Table 4.2.1.4: Abutment on Ganga sand

Sl. No.	Embedment Depth Ratio H_E/D	Flow Depth Ratio h/D	Scour Depth Ratio hs/D	Discharge m^3/Sec/m	Velocity (m/sec) V	Froude No. F_R	Experimental Observations $(G_f/h)_e$	Theoretical Prediction $(G_f/h)_t$	Goodness Ratio $\frac{(G_f/h)_t}{(G_f/h)_e}$
1	1	2.024	0.688	0.02904	0.2869	0.288	0.1541	0.4799	3.11
2	1.5	2.04	1.046	0.03075	0.3015	0.3014	0.2225	0.4971	2.23
3	1.75	2.056	1.156	0.03438	0.3344	0.3330	0.2889	0.5372	1.86
4	2	2.066	1.288	0.03729	0.3610	0.3586	0.3446	0.5693	1.65
5	2.5	2.2	1.634	0.04119	0.3744	0.3604	0.3936	0.5697	1.44
6	3	2.28	2.048	0.04371	0.3835	0.3626	0.4175	0.5713	1.36
7	3.5	2.51	2.296	0.05059	0.4031	0.3632	0.4796	0.5692	1.18

Table 4.2.1.5: Circular pier on Ganga sand

Sl. No.	Embedment Depth Ratio H_E/D	Flow Depth Ratio h/D	Scour Depth Ratio hs/D	Discharge m^3/Sec/m	Velocity (m/sec) V	Froude No. F_R	Experimental Observations $(G_f/h)_e$	Theoretical Prediction $(G_f/h)_t$	Goodness Ratio $\frac{(G_f/h)_t}{(G_f/h)_e}$
1	1	2.06	0.748	0.03009	0.2921	0.2906	0.1223	0.4829	3.95
2	1.5	2.126	0.996	0.03367	0.3167	0.3101	0.2370	0.5072	2.14
3	1.75	2.11	1.086	0.03715	0.3521	0.3462	0.3146	0.553	1.75
4	2	2.272	1.224	0.04521	0.3980	0.3770	0.3415	0.5894	1.72
5	2.5	2.636	1.532	0.05702	0.4326	0.3804	0.3672	0.5889	1.60
6	3	2.86	1.756	0.06478	0.4530	0.3825	0.4349	0.5888	1.35

Table 4.2.1.6: Oblong pier on Ganga sand

Sl. No.	Embedment Depth Ratio H_E/D	Flow Depth Ratio h/D	Scour Depth Ratio hs/D	Discharge m^3/Sec/m	Velocity (m/sec) V	Froude No. F_R	Experimental Observations $(G_f/h)_e$	Theoretical Prediction $(G_f/h)_t$	Goodness Ratio $\frac{(G_f/h)_t}{(G_f/h)_e}$
1	1	2.02	0.776	0.02888	0.2859	0.2873	0.1108	0.4791	4.32
2	1.5	2.024	1.044	0.03322	0.3283	0.3295	0.2252	0.5331	2.36
3	1.75	2.086	1.12	0.03639	0.3489	0.3449	0.3020	0.5518	1.82
4	2	2.278	1.242	0.04218	0.3703	0.3503	0.3327	0.556	1.67
5	2.5	2.28	1.664	0.0434	0.3807	0.36	0.3666	0.568	1.55
6	3	2.35	1.892	0.04704	0.4004	0.3729	0.4714	0.5832	1.23
7	3.5	2.474	2.292	0.05097	0.4121	0.3741	0.4882	0.583	1.19

Table 4.2.1.5: Circular pier on Ganga sand

Sl. No.	Embedment Depth Ratio H_E/D	Flow Depth Ratio h/D	Scour Depth Ratio hs/D	Discharge m^3/Sec/m	Velocity (m/sec) V	Froude No. F_R	Experimental Observations $(G_f/h)_e$	Theoretical Prediction $(G_f/h)_t$	Goodness Ratio $\frac{(G_f/h)_t}{(G_f/h)_e}$
1	1	2.06	0.748	0.03009	0.2921	0.2906	0.1223	0.4829	3.95
2	1.5	2.126	0.996	0.03367	0.3167	0.3101	0.2370	0.5072	2.14
3	1.75	2.11	1.086	0.03715	0.3521	0.3462	0.3146	0.553	1.75
4	2	2.272	1.224	0.04521	0.3980	0.3770	0.3415	0.5894	1.72
5	2.5	2.636	1.532	0.05702	0.4326	0.3804	0.3672	0.5889	1.60
6	3	2.86	1.756	0.06478	0.4530	0.3825	0.4349	0.5888	1.35

Table 4.2.1.6: Oblong pier on Ganga sand

Sl. No.	Embedment Depth Ratio H_E/D	Flow Depth Ratio h/D	Scour Depth Ratio hs/D	Discharge m^3/Sec/m	Velocity (m/sec) V	Froude No. F_R	Experimental Observations $(G_f/h)_e$	Theoretical Prediction $(G_f/h)_t$	Goodness Ratio $\frac{(G_f/h)_t}{(G_f/h)_e}$
1	1	2.02	0.776	0.02888	0.2859	0.2873	0.1108	0.4791	4.32
2	1.5	2.024	1.044	0.03322	0.3283	0.3295	0.2252	0.5331	2.36
3	1.75	2.086	1.12	0.03639	0.3489	0.3449	0.3020	0.5518	1.82
4	2	2.278	1.242	0.04218	0.3703	0.3503	0.3327	0.556	1.67
5	2.5	2.28	1.664	0.0434	0.3807	0.36	0.3666	0.568	1.55
6	3	2.35	1.892	0.04704	0.4004	0.3729	0.4714	0.5832	1.23
7	3.5	2.474	2.292	0.05097	0.4121	0.3741	0.4882	0.583	1.19

Table 4.2.1.7: Mamgain (2001) data of circular pier on Yamuna sand

Sl. No.	Embedment Depth Ratio H_E/D	Flow Depth Ratio h/D	Scour Depth Ratio hs/D	Discharge m^3/Sec/m	Velocity (m/sec) V	Froude No. F_R	Experimental Observations $(G_f/h)_e$	Theoretical Prediction $(G_f/h)_t$	Goodness Ratio $\frac{(G_f/h)_t}{(G_f/h)_e}$
1	1.5	2.4713	1.138	0 .0317	0.2565	0.233	0.1468	0.4105	2.80
2	1.75	2.6333	1.28	0.0372	0.2822	0.2483	0.1784	0.429	2.40
3	2	2.688	1.276	0.0391	0.2910	0.2534	0.2693	0.4351	1.61
4	2.25	2.99	1.34	0.0510	0.3414	0.2819	0.3043	0.4689	1.54
5	2.5	3.174	1.42	0.0687	0.4327	0.3174	0.3402	0.5121	1.50
6	2.75	3.3293	1.635	0.0668	0.4011	0.3139	0.3349	0.5061	1.51
7	3	3.3827	1.846	0.0695	0.4108	0.3189	0.3411	0.5119	1.50

TABLE 4.2.2: Experimental observation and theoretical prediction for model 2

Table 4.2.2.1: Abutment on Yamuna sand

Sl. No.	Embedment Depth Ratio H_E/D	Flow Depth Ratio h/D	Scour Depth Ratio hs/D	Discharge m^3/Sec/m	Velocity (m/sec) V	Froude No. F_R	Experimental Observations $(G_f/h)_e$	Theoretical Prediction $(G_f/h)_t$	Goodness Ratio $\frac{(G_f/h)_t}{(G_f/h)_e}$
1	1	2.082	0.736	0.0272	0.2622	0.2595	0.12680	0.4494	3.54
2	1.5	2.062	1.08	0.0278	0.2705	0.2690	0.20368	0.4622	2.26
3	1.75	2.106	1.212	0.0322	0.3063	0.3014	0.25546	0.5042	1.97
4	2	2.098	1.344	0.0329	0.3144	0.31	0.31267	0.5155	1.64
5	2.5	2.136	1.75	0.0353	0.3310	0.3234	0.35112	0.5323	1.51
6	3	2.32	2.128	0.0410	0.3541	0.3320	0.37586	0.5408	1.43
7	3.5	2.51	2.434	0.0489	0.3902	0.3517	0.42470	0.5634	1.32
8	4	2.74	2.62	0.05781	0.4224	0.3644	0.50365	0.5764	1.14

Table 4.2.2.2: Circular pier on Yamuna sand

Sl. No.	Embedment Depth Ratio H_E/D	Flow Depth Ratio h/D	Scour Depth Ratio hs/D	Discharge m^3/Sec/m	Velocity (m/sec) V	Froude No. F_R	Experimental Observations $(G_f/h)_e$	Theoretical Prediction $(G_f/h)_t$	Goodness Ratio $\frac{(G_f/h)_t}{(G_f/h)_e}$
1	1	2.106	0.764	0.03032	0.2879	0.2833	0.11206	0.4805	4.28
2	1.5	2.084	1.13	0.03394	0.3257	0.3221	0.17754	0.5314	2.99
3	1.75	2.094	1.16	0.03564	0.3404	0.3358	0.28175	0.549	1.94
4	2	2.3	1.25	0.041986	0.3650	0.3437	0.32608	0.5561	1.70
5	2.5	2.64	1.59	0.05398	0.4089	0.3593	0.34469	0.5713	1.65
6	3	2.8	1.892	0.05956	0.4254	0.3630	0.39571	0.5739	1.45

Table 4.2.2.3: Oblong pier on Yamuna sand

Sl. No.	Embedment Depth Ratio H_E/D	Flow Depth Ratio h/D	Scour Depth Ratio hs/D	Discharge m^3/Sec/m	Velocity (m/sec) V	Froude No. F_R	Experimental Observations $(G_f/h)_e$	Theoretical Prediction $(G_f/h)_t$	Goodness Ratio $\frac{(G_f/h)_t}{(G_f/h)_e}$
1	1	2.076	0.788	0.02930	0.2823	0.2797	0.1021	0.4763	4.66
2	1.5	2.094	1.068	0.03088	0.2950	0.2911	0.2063	0.4909	2.37
3	1.75	2.044	1.128	0.03185	0.3117	0.3113	0.3043	0.518	1.70
4	2	2.07	1.296	0.03377	0.3263	0.3238	0.3400	0.5338	1.56
5	2.5	2.16	1.69	0.03739	0.3462	0.3363	0.375	0.5486	1.46
6	3	2.28	1.996	0.04108	0.3604	0.3408	0.4403	0.5526	1.25
7	3.5	2.69	2.248	0.05524	0.4107	0.3575	0.4654	0.5684	1.22
8	4	3.01	2.548	0.06778	0.4504	0.3707	0.48239	0.581	1.20

Table 4.2.2.4: Abutment on Ganga sand

Sl. No.	Embedment Depth Ratio H_E/D	Flow Depth Ratio h/D	Scour Depth Ratio hs/D	Discharge m^3/Sec/m	Velocity (m/sec) V	Froude No. F_R	Experimental Observations $(G_y/h)_e$	Theoretical Prediction $(G_y/h)_t$	Goodness Ratio $\frac{(G_y/h)_t}{(G_y/h)_e}$
1	1	2.024	0.688	0.02904	0.2869	0.288	0.1541	0.4815	3.12
2	1.5	2.04	1.046	0.03075	0.3015	0.3014	0.2225	0.4986	2.24
3	1.75	2.056	1.156	0.03438	0.3344	0.3330	0.2889	0.5389	1.86
4	2	2.066	1.288	0.03729	0.3610	0.3586	0.3446	0.5711	1.65
5	2.5	2.2	1.634	0.04119	0.3744	0.3604	0.3936	0.5717	1.45
6	3	2.28	2.048	0.04371	0.3835	0.3626	0.4175	0.5734	1.37
7	3.5	2.51	2.296	0.05059	0.4031	0.3632	0.4796	0.5715	1.19

Table 4.2.2.5: Circular pier on Ganga sand

Sl. No.	Embedment Depth Ratio H_E/D	Flow Depth Ratio h/D	Scour Depth Ratio hs/D	Discharge m^3/Sec/m	Velocity (m/sec) V	Froude No. F_R	Experimental Observations $(G_y/h)_e$	Theoretical Prediction $(G_y/h)_t$	Goodness Ratio $\frac{(G_y/h)_t}{(G_y/h)_e}$
1	1	2.06	0.748	0.03009	0.2921	0.2906	0.1223	0.4845	3.96
2	1.5	2.126	0.996	0.03367	0.3167	0.3101	0.2370	0.5089	2.14
3	1.75	2.11	1.086	0.03715	0.3521	0.3462	0.3146	0.5548	1.76
4	2	2.272	1.224	0.04521	0.3980	0.3770	0.3415	0.5915	1.73
5	2.5	2.636	1.532	0.05702	0.4326	0.3804	0.3672	0.5914	1.61
6	3	2.86	1.756	0.06478	0.4530	0.3825	0.3864	0.5910	1.53

Table 4.2.2.6: Oblong pier on Ganga sand

Sl. No.	Embedment Depth Ratio H_E/D	Flow Depth Ratio h/D	Scour Depth Ratio hs/D	Discharge m^3/Sec/m	Velocity (m/sec) V	Froude No. F_R	Experimental Observations $(G_f/h)_e$	Theoretical Prediction $(G_f/h)_t$	Goodness Ratio $\frac{(G_f/h)_t}{(G_f/h)_e}$
1	1	2.02	0.776	0.02888	0.2859	0.2873	0.1108	0.4806	4.33
2	1.5	2.024	1.044	0.03322	0.3283	0.3295	0.2252	0.5347	2.37
3	1.75	2.086	1.12	0.03639	0.3489	0.3449	0.3020	0.5536	1.83
4	2	2.278	1.242	0.04218	0.3703	0.3503	0.3327	0.5581	1.67
5	2.5	2.28	1.664	0.0434	0.3807	0.36	0.3666	0.5701	1.55
6	3	2.35	1.892	0.04704	0.4004	0.3729	0.4714	0.5854	1.24
7	3.5	2.474	2.292	0.05097	0.4121	0.3741	0.4882	0.5854	1.19

Table 4.2.2.7: Mamgain (2001) data of circular pier on Yamuna sand

Sl. No.	Embedment Depth Ratio H_E/D	Flow Depth Ratio h/D	Scour Depth Ratio hs/D	Discharge m^3/Sec/m	Velocity (m/sec) V	Froude No. F_R	Experimental Observations $(G_f/h)_e$	Theoretical Prediction $(G_f/h)_t$	Goodness Ratio $\frac{(G_f/h)_t}{(G_f/h)_e}$
1	1.5	2.4713	1.138	0 .0317	0.2565	0.233	0.1468	0.4163	2.84
2	1.75	2.6333	1.28	0.0372	0.2822	0.2483	0.1784	0.4351	2.43
3	2	2.688	1.276	0.0391	0.2910	0.2534	0.2693	0.4413	1.63
4	2.25	2.99	1.34	0.0510	0.3414	0.2819	0.3043	0.4754	1.56
5	2.5	3.174	1.42	0.0687	0.4327	0.3174	0.3402	0.5191	1.52
6	2.75	3.3293	1.635	0.0668	0.4011	0.3139	0.3349	0.5128	1.53
7	3	3.3827	1.846	0.0695	0.4108	0.3189	0.3411	0.5186	1.52

4.3 Results and Discussion

For both the model using the final expression for them (equation 4.7 and 4.10), the value of ratio of grip length to flow depth (G_l/h) are computed for different h/D, h_s/D, H_E/D, F_R^2, d_{50} and Lacey's silt factor f values. In Table 4.2.1 computed value of G_l/h are presented and value obtained by experimental observations are also presented in the same table for the first model. In Table 4.2.2 computed value of G_l/h and its corresponding experimental value is presented for second model. The correctness of predicted values of G_l/h with respect to the experimental observations is measured in terms of a Goodness ratio defined as the ratio of the theoretical prediction of the same to the experimental observed values. From the Table 4.2.1 and 4.2.2 it is clear that Goodness ratio is close to unity for embedment depth ratio (H_E/D) greater than 2. But for embedment depth ratio less than 2, Goodness ratio is not very satisfactory for both the model. It is seen from the Table 4.2.1 and Table 4.2.2 that fine sand gives better Goodness ratio than coarse sand. This semi-empirical theory can be used for predicting the grip length when embedment depth ratio is greater than 2. But for embedment depth ratio less than 2, this theory gives error so it should not be used for H_E/D value less than 2.

CHAPTER 5

CONCLUSIONS

The major conclusions of the study are as follows:

1. Parameters indicating scour depth and embedment depth bears a linear relationship with each other. The relation being $y = 0.699x + 0.6042$, where $y = (h+h_s)/D$ and $x = (h+H_E)/D$. The correlation coefficient (R) is approximately equal to 1, indicating excellent predictions can be achieved using the above relation. The expression is valid for Froude number ranging from 0.2595 to 0.3825.

2. Ratio of scour depth to embedment depth [$y = \{(h+h_s)/(h+H_E)\}$] bears a non-linear relationship with the ratio of discharge intensity and pier diameter [$x = q/(gD^3)^{1/2}$] as follows having a coefficient of correlation (R) equals to 0.84, The relationship is $y = 0.8573x^{-0.1606}$.

3. Ratio of scour depth to embedment depth as defined above [$y = \{(h+h_s)/(h+H_E)\}$] with Froude number (x) bears a non-linear relationship, the relation is $y = 0.5344x^{-0.4116}$. The coefficient of correlation (R) is 0.90.

4. Ratio of grip length to embedment depth [$y = \{(H_E-h_s)/(h+H_E)\}$] bears a nonlinear relationship with Froude number (x) for both (Yamuna and Ganga) sand combined. The relationship is $y = 2.6549x^{2.5966}$ and the correlation coefficient is 0.87.

5. The developed predicted model gives good results in terms with experimental values for both piers and abutments so long the embedment depth ratio (H_E/D) is greater than 2. The goodness ratio varies from 1.13 to 1.67. But when the embedment depth ratio (H_E/D) is less than 2 the prediction is very poor.

6. For developed semi empirical theory, fine sand gives better Goodness ratio than coarse sand.

5.1 Suggestions for further studies

Based on the present work on Yamuna and Ganga sand, the following aspect of work are suggested for further studies:

1. Present study may be focused towards the scouring pattern in stratified soil deposits.
2. An effort can be made to improve the proposed theory, when the grip length ratio H_E/D is less than 2.
3. Similar experiments can be done for the grip length measurement at limiting equilibrium for large range of H_E/D values for silt, silt-clay deposits.

REFRENCES

1. Baker, C. J. (1981), "New Design Equation for Scour around Bridge Piers", Jr. of Hydraulic Division, Proc. ASCE, Vol. 107 (HY –4).

2. Baker, R. E. (1986), "Local Scour at Bridge Piers in Non-uniform sediment", Rep. No. 402, School of Engg., The University of Auckland, New Zealand.

3. Barnard, S. and Child, J. M. (1994), "Higher Algebra", Macmillan Publishers, pp.-180.

4. Breusers, H.N.C., Nicollet, G., and Shen, H.W. (1977), "Local Scour around Cylindrical Piers", J. Hydraulics Res., Vol. 15(3) : 211-252.

5. Chiew, Y.M. (1984), "Local Scour at Bridge Piers", Ph.D. Thesis, The Univ. of Auckland, Auckland, New Zealand.

6. Dongal, D.M.S. (1994), "Local Scour at Bridge Abutments", Rep. No. 544, School of Engg., The Univ. of Auckland, New Zealand.

7. Ettema, R. (1980), "Scour at Bridge Sites", Rep. No. 117, Univ. of Auckland, Auckland, New Zealand.

8. Jones et al. (1993), "Preliminary Studies of Pressure Flow Scour", ASCE Hydraulic Engg., Proc. National conference, San Francisco.

9. Kothyari, U.C. (1989), "Scour Around Bridge Piers", Ph.D. Thesis, Univ. of Roorkee, India.

10. Laursen, E. M. and Toch, A. (1956), "Scour Around Bridge Piers and Abutments; Iowa Highway Res. Board, Bulletin No. 4, pp. 60.

11. Laursen, E. M. (1963), "Analysis of Bridge Scour", J. Hydr. Div., ASCE, Vol. 89(3), 93 - 118.

12. Mamgain, P. (2001), "Scour Around River Crossing Pile Foundations", Masters Thesis, Indian Institute of Technology, Kanpur

13. Melville, B W (1997), "Peir and Abutment Scouring: Integrated Approach", Jr. Hydr Engg., ASCE, Vol. 123(2): 125-135.

14. Melville, B W. (1998), "Effects of Pier Shape on local Scour", Jr. of Water Resource Engg., ASCE

15. Melville, B W. (1992), " Local Scour at Bridge Abutment", Jr. Hydr. Engg., Proc. ASCE, Vol 118(4): 615-631.

16. Melville, B W. (1975), "Local Scour at Bridge Sites", Rep. No. 117, Univ. of Auckland, Auckland, New Zealand.

17. Melville, B W. (1988), " Scour at Bridge sites", Chapter 15, Civil Engineering Practice, Ed. P.N. Cheremisinoff, San Ling Chang.

18. Muzzammil, M. and Gangadharaiah, at. (1995), "A Study of Scouring Horseshoe Vortex", 6th International Symposium in River Sedimentation, New Delhi, Nov. 7-11: 923-943

19. Raudkivi, A. J., and Ettema, R. (1977), "Effect of Sediment Gradation on Clear Water Scour", Jr. Hydr. Div., ASCE, Vol. 103(10): 1209-1212.

20. Raudviki, A. J. (1990), "Loose Boundary Hydraulics", Pergamon Press.